nature plants

Article

https://doi.org/10.1038/s41477-023-01514-w

A transcription factor *ZmGLK36* confers broad resistance to maize rough dwarf disease in cereal crops

Received: 26 October 2022

Accepted: 7 August 2023

Published online: 14 September 2023

Check for updates

Zhennan Xu[1,9], Zhiqiang Zhou[1,9], Zixiang Cheng[1], Yu Zhou[2], Feifei Wang[1], Mingshun Li[1], Gongjian Li[1], Wenxue Li[1], Qingguo Du[1], Ke Wang[1], Xin Lu[1], Yuxin Tai[1], Runyi Chen[1], Zhuanfang Hao[1], Jienan Han[1], Yanping Chen[3], Qingchang Meng[3], Xiaomin Kong[4], Shuanggui Tie[5], Chunhua Mu[6], Weibin Song[7], Zhenhua Wang[2], Hongjun Yong[1], Degui Zhang[1], Haiyang Wang[8] ✉, Jianfeng Weng[1] ✉ & Xinhai Li[1] ✉

Maize rough dwarf disease (MRDD), caused by maize rough dwarf virus (MRDV) or rice black-streaked dwarf virus (RBSDV), seriously threatens worldwide production of all major cereal crops, including maize, rice, wheat and barley. Here we report fine mapping and cloning of a previously reported major quantitative trait locus (QTL) (*qMrdd2*) for RBSDV resistance in maize. Subsequently, we show that *qMrdd2* encodes a G2-like transcription factor named *ZmGLK36* that promotes resistance to RBSDV by enhancing jasmonic acid (JA) biosynthesis and JA-mediated defence response. We identify a 26-bp indel located in the 5′ UTR of *ZmGLK36* that contributes to differential expression and resistance to RBSDV in maize inbred lines. Moreover, we show that ZmDBF2, an AP2/EREBP family transcription factor, directly binds to the 26-bp indel and represses *ZmGLK36* expression. We further demonstrate that *ZmGLK36* plays a conserved role in conferring resistance to RBSDV in rice and wheat using transgenic or marker-assisted breeding approaches. Our results provide insights into the molecular mechanisms of RBSDV resistance and effective strategies to breed RBSDV-resistant cereal crops.

Plant virus diseases, often called 'plant cancers', have long been a major obstacle to agricultural production worldwide, causing billions of dollars in damage to global crop production annually[1,2]. Rice black-streaked dwarf virus (RBSDV) and maize rough dwarf virus (MRDV) are closely related members of the *Fijivirus* genus in *Reoviridae* and they can infect almost all major cereal crops in Asia, Europe and South America, including maize, rice, wheat, barley and other cereal crops. While MRDV primarily infects maize in Europe and South America, RBSDV mainly infects maize in Asia, causing maize rough dwarf disease (MRDD), which is characterized by dwarfing of plants, shortening of internodes, thickened, short and stiff green leaves, and ultimately results in heavy yield losses (ranging from 30% to 100%)[3,4]. RBSDV and MRDV are

[1]State Key Laboratory of Crop Gene Resources and Breeding, Institute of Crop Sciences, Chinese Academy of Agricultural Sciences, Beijing, China. [2]Northeast Agricultural University, Harbin, China. [3]Jiangsu Academy of Agricultural Sciences, Nanjing, China. [4]Jining Academy of Agricultural Sciences, Jining, China. [5]Henan Academy of Agricultural Sciences, Zhengzhou, China. [6]Shandong Academy of Agricultural Sciences, Jinan, China. [7]China Agricultural University, Beijing, China. [8]Guangdong Laboratory for Lingnan Modern Agriculture, State Key Laboratory for Conservation and Utilization of Subtropical Agro-Bioresources, South China Agricultural University, Guangzhou, China. [9]These authors contributed equally: Zhennan Xu, Zhiqiang Zhou. ✉e-mail: whyang@scau.edu.cn; wengjianfeng@caas.cn; lixinhai@caas.cn

transmitted in a persistent manner by the small brown planthopper (SBPH, *Laodelphax striatellus*)[5–8]. Although adjustment of the sowing dates and chemical agents are commonly used to alleviate the disease and yield loss caused by RBSDV or MRDV, these practices are inefficient and harmful to the environment. Therefore, breeding of MRDD-resistant cultivars has remained the most effective and environment-friendly approach for management of the viral diseases[4,9].

Resistance to RBSDV and MRDV is a complex genetic trait controlled by multiple loci and easily affected by the environment[10–13]. Extensive genetic studies based on genome-wide association studies or linkage mapping have led to the identification of over 30 quantitative trait loci (QTLs) for RBSDV or MRDV resistance[10–12,14–22]; however, only 3 genes conferring RBSDV resistance have been cloned and functionally characterized in plants. It was shown that *aspartic proteinase 47* (*OsAP47*) and Golden 2-like 1 (*OsGLK1*) respectively underlie *qRBSDV6-1* and *qRBSDV6* in rice and that their high expression confers susceptibility and resistance, respectively[21,22]. In maize, it was shown that the Rab GDP dissociation inhibitor alpha (RabGDIα) underlies *qMrdd8* and that it acts as a host susceptibility factor for RBSDV. The viral RBSDV-P7-1 protein binds to exon 10 and the C terminus of the susceptible-type ZmGDIα to facilitate virus replication, whereas insertion of a helitron transposon into the resistant-type RabGDIα intron 10 causes alternative splicing of exon 10, thus weakening the binding of the P7-1 protein to RabGDIα-hel[20]. Nevertheless, due to the limited effects of individual loci on RBSDV resistance (typically less than 10% phenotypic variance), it remains an imperative task to isolate more RBSDV resistance genes, especially ones that could confer broad resistance in all major cereal crops and without apparent detrimental effects on other agronomic traits.

The plant hormone jasmonate (JA) and its derivatives are well known for their role in regulating plant responses to abiotic stresses and defence against pathogen infection[23–28]. The JA signalling cascade has been well illustrated in the model plant *Arabidopsis thaliana*, including identification and functional studies of the jasmonic acid receptor (COI1) and key signalling components, such as the mediator subunit MED25, JAZ repressors and MYC transcription factors[23,29,30]. Recent studies have shown a host–virus arms race during evolution. On one hand, viral RNA could be recognized by the host's surveillance system to activate the plant RNA silencing machinery, thus triggering broad-spectrum disease resistance[29]. On the other hand, viruses have evolved a variety of different strategies to attack the plant's antiviral equipment and escape the plant's defence response. For example, rice viruses in the genera *Fijivirus*, *Tenuivirus* and *Cytorhabdovirus* all encode viral proteins that could act as transcriptional repressors to hijack and repress the host JA pathway to benefit viral infection and the feeding behaviour of vector insects[31]. Despite the progress made in this area of research, however, the role of JA and the regulatory mechanisms of RBSDV resistance have remained largely unknown in cereal crops.

In this study, we cloned a major QTL for RBSDV resistance in maize and demonstrate that it enhances RBSDV resistance by directly enhancing the expression of JA biosynthesis genes. We identify ZmDBF2 as an upstream transcription factor that represses *ZmGLK36* expression in maize inbred lines and demonstrate that *ZmGLK36* is effective in conferring broad resistance to RBSDV in rice and wheat.

Result

Characteristics of MRDD symptoms

We previously reported the identification of *qMrdd2*, a major QTL for RBSDV resistance in maize (explaining 8.64% to 11.02% of the total phenotypic variance), using recombinant inbred lines (RILs) and chromosomal segment substitution lines derived from a cross between the maize inbred Qi319 as the MRDD resistance donor and Ye478 as the susceptible recipient[12] (Extended Data Fig. 1a). To facilitate cloning of this locus, we developed a pair of near-isogenic line (NIL) called NIL-S and NIL-R (Fig. 1a). Inoculation assay verified that the NIL-R had much stronger resistance to RBSDV, as illustrated by the significantly lower accumulation of *RBSDV-S10* RNA levels in NIL-R than in NIL-S based on real time quantitative PCR (RT–qPCR) assay (Extended Data Fig. 1b). We further examined the field phenotypes of NIL-S and NIL-R. After artificial inoculation of RBSDV at the V3 stage, MRDD severity at the silking stage could be classified into five grades (0, 1, 2, 3 and 4) in view of the overall symptoms at the mature stage based on plant height and the characteristics of the lesions (Extended Data Fig. 1c–e). Plants with the most severe symptoms (disease grade 4) had only 8 internodes, whereas plants of other disease grades (0–3) had 15 internodes (Extended Data Fig. 1f). Cellular examination of the 8th internode of the grade 4 plants revealed that cell elongation was much suppressed in the NIL-S compared with the NIL-R plants (Extended Data Fig. 1g,h). Moreover, we observed that the NIL-S plants developed abnormal vascular bundles, characterized by an atrophied xylem (Extended Data Fig. 1g).

qMrdd2 encodes ZmGLK36

qMrdd2 was previously fine mapped to a 315-kb interval on maize chromosome 2 (ref. 12) (Fig. 1b). This region contains nine annotated genes according to the B73_V4 reference genome. To determine the precise genetic variation between the two parental lines, we de novo assembled high-quality genomes of Qi319 and Ye478 using long-read sequencing technologies (see online Methods and Supplementary Table 1). Sequence alignment showed that in the mapped 315-kb interval, both Qi319 and Ye478 had the same nine annotated genes as B73 (Fig. 1b). Sequence analysis revealed that among the nine genes, *Zm00001d002433*, *Zm00001d002436* and *Zm00001d002439* have structural variation in addition to single nucleotide polymorphism (SNP) variations between Qi319 and Ye478. To identify the responsible gene, we conducted RT–qPCR analysis of these candidate genes in the NIL-R and NIL-S lines at 12 day post infection (dpi) with RBSDV. Among the candidate genes, only the expression of *Zm00001d002439* (encoding G2-like transcription factor 36, *ZmGLK36*) was significantly induced by RBSDV in NIL-R (Fig. 1c and Extended Data Fig. 2). It started to accumulate at 1.5 dpi, peaked at 6 to 12 dpi and then subsided to near the basal level within 48 dpi in NIL-R. Intriguingly, *Zm00001d002439* showed an opposite expression trend after inoculation with RBSDV in NIL-S (Fig. 1c).

Fig. 1 | Map-based cloning of *ZmGLK36*. **a**, MRDD phenotypes of the NIL-R and NIL-S lines. Scale bar, 35 cm. **b**, Fine mapping of *qMrdd2*. Top: the position of *qMrdd2*. Middle: the markers. Bottom: the 9 candidate genes in the mapped region. **c**, Relative expression levels of *ZmGLK36* in NIL-R and NIL-S. The plants were artificially inoculated at the V3 stage. Data are means ± s.e.m. ($n = 3$ biologically independent samples with 5 plants per biological replicate). **d**,**g**, MRDD phenotypes of Zong31, #-1$^{ZmGLK36\text{-}Qi319}$, #-2$^{ZmGLK36\text{-}Qi319}$, #-3$^{ZmGLK36\text{-}Qi319}$, KO-1^{ZmGLK36} and KO-2^{ZmGLK36} under indicated treatments. **e**,**h**, DSI values of the transgenic complementary and knockout plants at the silking stage. The plants were artificially inoculated at the V3 stage. Data are means ± s.e.m. from 3 biological replicates ($n = 60$ plants per replicate). **f**,**i**, The relative expression of RBSDV coat protein (S10) mRNA at the silking stage. The plants were artificially inoculated at the V3 stage. The number of samples is the same as that in **c**. Data are means ± s.e.m. from 3 biological replicates ($n = 5$ plants per replicate). **j**, *ZmGLK36*-based association mapping and pairwise LD analysis. Triangles denote indels and dots represent SNPs. Red lines highlight the strong LD of indel-26 with the significant variants. **k**, Haplotypes of *ZmGLK36* among 97 maize lines. *n* denotes the number of maize lines. Statistical significance was determined using a two-sided *t*-test. **l**, Comparison of *ZmGLK36* expression between Hap 1 and Hap 2 after artificial inoculation with RBSDV at 12 dpi. The gene expression level was determined among 23 maize inbred lines. Data are means ± s.e.m. from 3 biological replicates ($n = 5$ plants per replicate). Exact *P* values are shown; two-sided Student's *t*-test. In **j**, *P* values were determined under the mixed linear model using Wald test, implemented in GEMMA.

https://doi.org/10.1038/s41477-023-01514-w

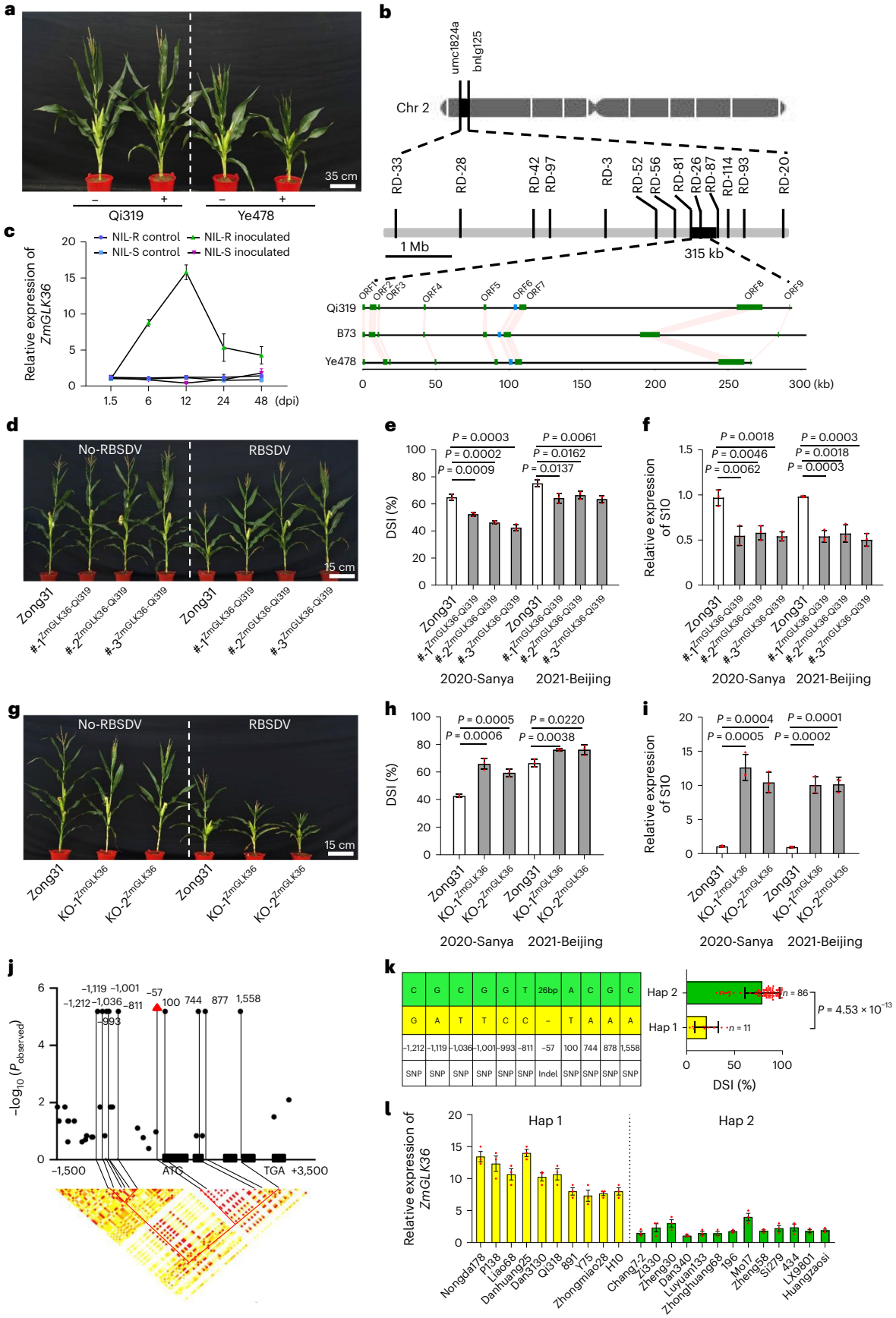

To test whether *ZmGLK36* represents *qMrdd2*, we transformed a genomic DNA fragment containing the 3-kb intact coding region and 2-kb promoter region of *ZmGLK36* from Qi319 into the susceptible recipient Zong31. Three independent transgenic events (#-1$^{ZmGLK36\text{-}Qi319}$, #-2$^{ZmGLK36\text{-}Qi319}$ and #-3$^{ZmGLK36\text{-}Qi319}$) were obtained. Inoculation assay showed that the disease severity index (DSI) and *RBSDV-S10* expression level were significantly lower in all three transgenic lines than in Zong31 (Fig. 1d–f). In addition, we generated two independent *ZmGLK36* knockout lines (KO-1^{ZmGLK36} and KO-2^{ZmGLK36}) in Zong31 background using the CRISPR/Cas9 technology (Extended Data Fig. 3a–c). As expected, the knockout lines exhibited greater susceptibility and higher *RBSDV-S10* expression level compared with Zong31 (Fig. 1g–i). These results confirm that *ZmGLK36* is responsible for RBSDV resistance.

ZmGLK36 encodes a transcription factor belonging to the GARP superfamily (Extended Data Fig. 4a). RT–qPCR assay showed that it was ubiquitously expressed in root, leaf, internode and embryo (Extended Data Fig. 4b). The expression pattern was further verified by histochemical staining of the transgenic plants carrying a β-glucuronidase (GUS) reporter driven by the endogenous *ZmGLK36* promoter (Extended Data Fig. 4c). RNA in situ hybridization revealed that *ZmGLK36* is preferentially expressed in vascular bundles (Extended Data Fig. 4d,e). Subcellular localization assay showed that the ZmGLK36 protein was predominantly localized to the nucleus, consistent with the function of a putative transcription factor (Extended Data Fig. 4f).

We next examined the genetic variation of *ZmGLK36* between Qi319 and Ye478. Sequence analysis revealed that there are 3 insertion/deletion (indels) and 13 SNPs in the complementary DNA of Qi319 and Ye478 (Extended Data Fig. 5). To test whether the genetic variations in the coding region play a role in MRDD resistance, we overexpressed the coding sequence (CDS) of ZmGLK36-Qi319 and ZmGLK36-Ye478 (both driven by the maize ubiquitin promoter) into Zong31. Six independent overexpression lines (OE-1$^{ZmGLK36\text{-}Qi319}$, OE-2$^{ZmGLK36\text{-}Qi319}$, OE-3$^{ZmGLK36\text{-}Qi319}$, OE-1$^{ZmGLK36\text{-}Ye478}$, OE-2$^{ZmGLK36\text{-}Ye478}$ and OE-3$^{ZmGLK36\text{-}Ye478}$) were obtained; the expression of *ZmGLK36* was increased by ~10 to 12 times in overexpression lines compared with Zong31 (Extended Data Fig. 6a). All six overexpression lines showed comparable and stronger resistance to MRDD and lower *RBSDV-S10* expression compared with Zong31 under artificial inoculation conditions (Extended Data Fig. 6b–e), suggesting that *ZmGLK36* functions as a positive regulator of resistance to MRDD and that the functional variations probably reside outside of the coding region of *ZmGLK36*.

To identify the causal variation of *ZmGLK36*, we sequenced the 5,100-bp genomic region, covering the promoter and gene coding regions of *ZmGLK36* in 97 maize inbred lines (Supplementary Table 2), and conducted association analysis of *ZmGLK36*. Ten SNPs and a 26-bp indel located in the 5′ untranslated regions (UTR) were found to be significantly associated with DSI (Fig. 1j). Notably, *ZmGLK36*-based association analysis showed that these sites are in complete linkage disequilibrium and they formed two haplotypes in 97 inbred lines (Hap 1 and Hap 2) (Fig. 1j,k). The *ZmGLK36*^{Qi319} allele is a representative of Hap 1 (n = 11), whereas the *ZmGLK36*^{Ye478} allele belongs to Hap 2 (n = 86). Statistically, the inbred lines with Hap 1 had a significantly lower DSI than the inbred lines with Hap 2 ($P = 4.53 \times 10^{-13}$) (Fig. 1k and Extended Data Fig. 7a). RT–qPCR assay showed that the expression of *ZmGLK36* was induced in the Hap 1 lines but suppressed in the Hap 2 lines upon inoculation with RBSDV (Fig. 1l). These results suggest that Hap 1 of the *ZmGLK36*^{Qi319} allele is inducible by RBSDV infection and that it confers resistance to MRDD.

Indel in 5′ UTR underlies *ZmGLK36* differential expression

Next, we performed a series of experiments to test whether the 26-bp indel in the 5′ UTR is associated with MRDD resistance. First, we randomly selected 10 resistant RILs and 10 susceptible RILs from the 314 RILs[32] for sequence analysis. The results showed that the 26-bp indel is in complete co-segregation with MRDD resistance (Extended Data Fig. 7b). Second, we randomly selected 6 lines that contain the *ZmGLK36*^{Qi319} allele (Hap 1) and 15 lines that contain the *ZmGLK36*^{Ye478} allele (Hap 2) on the basis of the 26-bp indel from 160 American maize inbred lines (Supplementary Table 3) and evaluated their RBSDV resistance. Field tests in both Jining (35.38° N, 116.59° E) and Beijing (40.13° N, 116.65° E) showed that the lines of Hap 1 had a significantly lower DSI than the inbred lines with Hap 2 (Extended Data Fig. 7c). To test whether the 26-bp indel is associated with *ZmGLK36* expression, we constructed two types of GUS reporter constructs. The GUS reporter gene was driven by the endogenous promoter of *ZmGLK36*^{Qi319} in one construct and by the endogenous promoter of *ZmGLK36*^{Qi319} plus the 26-bp indel (named *ZmGLK36*$^{Qi319+26}$; the 26-bp insertion was added to the Qi319 promoter by gene synthesis) in the other construct (Fig. 2a). Histochemical staining of the reporter transgenic lines showed that expression of *pZmGLK36*^{Qi319}::GUS, but not *pZmGLK36*$^{Qi319+26}$::GUS, was significantly induced at 12 dpi with RBSDV (Fig. 2b). This observation indicates that the 26-bp indel is involved in controlling the expression of *ZmGLK36* in response to RBSDV infection.

To substantiate the above notion, we used the CRISPR/Cas9 technology to delete the 26 bp in the 5′ UTR of *ZmGLK36*^{B73}, which has the same genotype as *ZmGLK36*^{Ye478}. We obtained a line (named KO-26) carrying the deletion of an 85-bp (encompassing the 26-bp indel) fragment in the 5′ UTR of *ZmGLK36*^{B73} (Extended Data Fig. 8a). As expected, reporter gene assay showed that the repressive activity of RBSDV on *ZmGLK36*^{B73} was significantly weakened by deleting the 85-bp indel, to a level comparable to that of the *ZmGLK36*^{Qi319} under artificial inoculation conditions (Fig. 2c and Extended Data Fig. 8b). Consistently, these transgenic plants were more resistant to RBSDV than the control plants B73, exhibiting a significant decrease in DSI and *RBSDV-S10* RNA levels (Fig. 2d,e and Extended Data Fig. 8c,d). Together, these observations verify that the 26-bp indel is a major causal variation underlying differential expression and resistance of *ZmGLK36* to RBSDV.

ZmDBF2 binds to 26 bp and represses the expression of *ZmGLK36*

To look for the upstream regulatory factors of *ZmGLK36*, we performed sequence analysis of the 26-bp indel in the 5′ UTR of *ZmGLK36*^{Ye478} via PlantPAN 3.0 TF (http://plantpan.itps.ncku.edu.tw/) and found that it contains binding sites for three transcription factors, including a

Fig. 2 | The 26-bp indel in the *ZmGLK36* promoter affects gene expression. **a**, Diagram of the *pZmGLK36*^{Qi319}::GUS and *pZmGLK36*$^{Qi319+26}$::GUS constructs. **b**, RT–qPCR shows the GUS mRNA levels at 12 dpi with RBSDV. Data are means ± s.e.m. (n = 3 biologically independent samples). Five plants were taken as one biological replicate (n = 5). **c**, Relative expression of *ZmGLK36* at 12 dpi with RBSDV. The number of samples is the same as that in **b**. Data are means ± s.e.m. **d**, DSI values of the KO-26 plants at the silking stage. The plants were artificially inoculated at the V3 stage. Data are means ± s.e.m. from 3 biological replicates (n = 40 plants per replicate). **e**, Relative expression of RBSDV coat protein (S10) at the silking stage. The plants were artificially inoculated at the V3 stage. Data are means ± s.e.m. from 3 biological replicates (n = 5 plants per replicate). **f**, Y1H assay shows that ZmDBF2 binds to the 26-bp fragment. **g**, Transient transcriptional activity assay in maize protoplast shows that ZmDBF2 represses the expression of *ZmGLK36*^{Ye478} by binding to the 26-bp fragment. Values are means ± s.e.m (n = 5 repeats). **h**, EMSA shows the binding of ZmDBF2 to the 26-bp fragment in the 5′ UTR of *ZmGLK36*^{Ye478}. Biotin-labelled probes and mutant probes are indicated in the bottom panel. Blue represents the binding motif and red represents the corresponding mutant sequence. **i**,**j**, MRDD phenotype of Zong31, OE-1^{ZmDBF2}, OE-2^{ZmDBF2}, OE-3^{ZmDBF2} and KO-1^{ZmDBF2}. **k**,**m**, DSI values of the transgenic overexpression and knockout plants for *ZmDBF2*. All plants were planted in Beijing and used for artificial inoculation. Data are means ± s.e.m. from 3 biological replicates (n = 50 plants per replicate). **l**,**n**, Relative expression of RBSDV coat protein (S10). Data are means ± s.e.m. from 3 biological replicates (n = 5 plants per replicate). Exact P values are shown; two-sided Student's t-test.

https://doi.org/10.1038/s41477-023-01514-w

binding site TCTCGCT for ZmDBF2 (an AP2/EREBP transcription factor), GCCTACC for ZmP1 (a Myb-like transcription factor) and GCTCGAGC for ZmbHLH74 (a putative HLH DNA-binding protein)[33,34]. Yeast one-hybrid assay (Y1H) showed that ZmDBF2 and ZmbHLH74, but not ZmP1, could directly bind to the 26-bp fragment (Fig. 2f and Extended Data Fig. 8e). Transient expression assay in maize protoplasts showed that ZmDBF2 exhibited significantly stronger repression on *pZmGLK36*^{Ye478} than on *pZmGLK36*^{Qi319} (Fig. 2g), suggesting that the 26-bp indel present

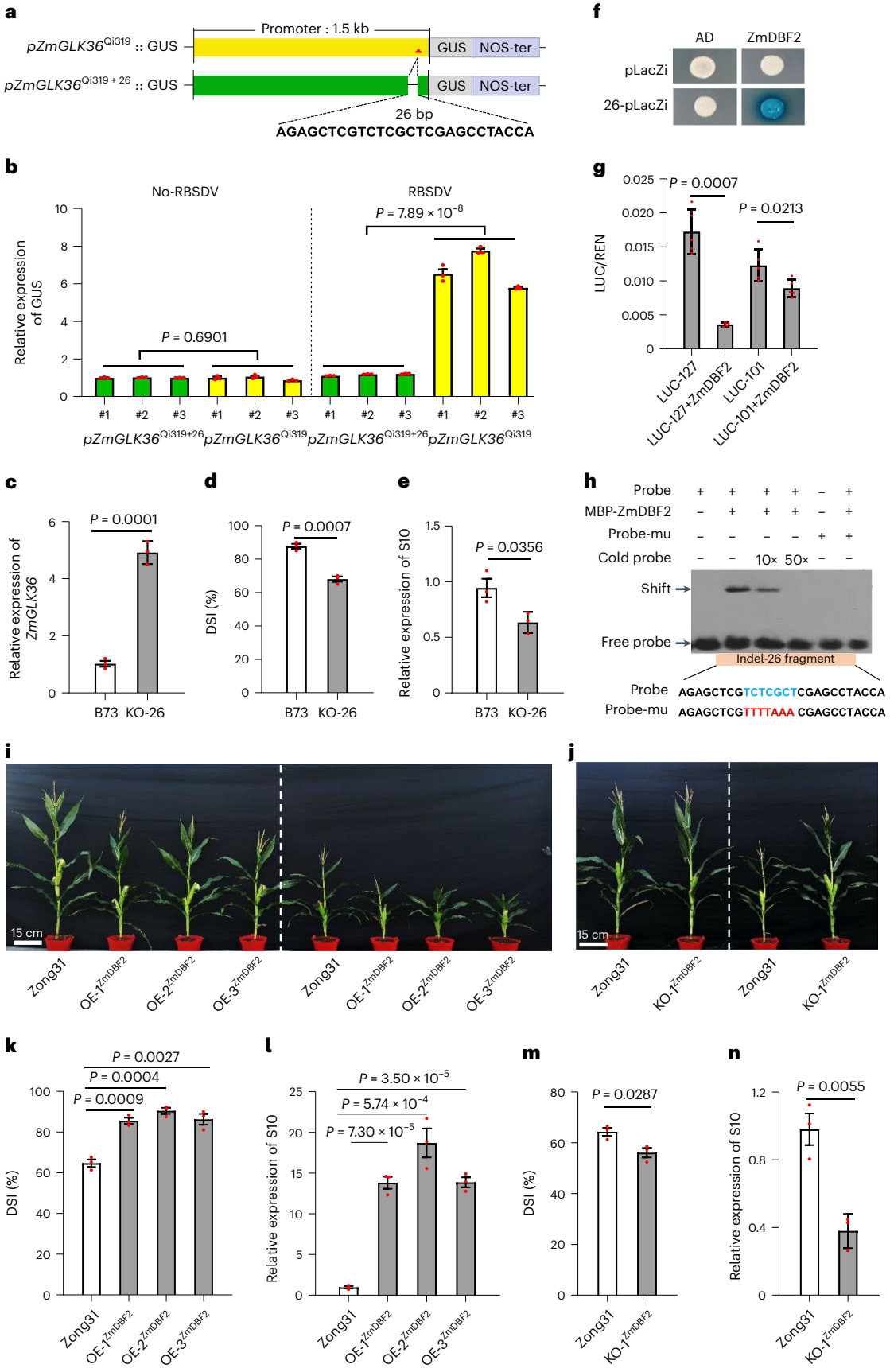

in the 5′ UTR of *ZmGLK36*^{Ye478} is probably responsible for recruiting a transcriptional repressor to suppress its expression. On the other hand, ZmbHLH74 activated the expression of *ZmGLK36*^{Ye478} (Extended Data Fig. 8f). RT–qPCR assay showed that the expression of both *ZmDBF2* and *ZmbHLH74* could be induced by RBSDV inoculation in both NIL-R and NIL-S (Extended Data Fig. 8g,h). Considering that *ZmGLK36*^{Qi319}, but not *ZmGLK36*^{Ye478}, could be induced by RBSDV, we speculated that the 26-bp indel in the promoter of *ZmGLK36*^{Ye478} is probably subject to transcriptional repression, hence ZmDBF2 was selected for further studies.

To test whether the predicted binding motif TCTCGCT is responsible for ZmDBF2 binding, we expressed and purified recombinant maltose binding protein (MBP)-ZmDBF2 fusion protein (Extended Data Fig. 8i,j) and used it for electrophoretic mobility shift assay (EMSA) assay. The 26-bp indel was labelled as the probe. The results showed that MBP-ZmDBF2 fusion protein could effectively slow down migration of the wild-type probe, but not the mutant probe in which the TCTCGCT motif was mutated into TTTTAAA (Fig. 2h). RT–qPCR assay showed that *ZmDBF2* was widely expressed in the root, leaf, internode and embryo (Extended Data Fig. 8k). To assess the functional role of *ZmDBF2*, we generated three overexpression lines (OE-1^{ZmDBF2}, OE-2^{ZmDBF2} and OE-3^{ZmDBF2}) (Fig. 2i) and one knockout line (Fig. 2j and Extended Data Fig. 8l) for *ZmDBF2* in the background of susceptible Zong31. As expected, all the *ZmDBF2*-overexpression lines showed significantly increased DSI and *RBSDV-S10* RNA levels compared with Zong31 (Fig. 2i,k,l). By contrast, the *Zmdbf2* knockout plants exhibited a significant decrease in DSI and *RBSDV-S10* RNA levels (Fig. 2j,m,n). RT–qPCR assay showed that expression of *ZmGLK36* was downregulated in the *ZmDBF2*-overexpressing plants but upregulated in the *Zmdbf2* knockout plants (Extended Data Fig. 8m). These results together demonstrate that ZmDBF2 is a negative regulator of RBSDV resistance and that it represses the expression of *ZmGLK36* through direct binding to (the TCTCGCT motif in) the 26-bp indel in the 5′ UTR of *ZmGLK36*.

The ZmGLK36–JA module confers resistance to RBSDV

Previous studies have shown that RBSDV can interact with host proteins to activate or inhibit host gene expression and accelerate virus replication[20,31]. Thus, we first used yeast two-hybrid (Y2H) assay to test for possible interactions between the 13 proteins of RBSDV and ZmGLK36. However, no direct interaction was detected (Extended Data Fig. 9). Subsequently, we performed RNA-sequencing and metabolomics-seq analyses of V3 stage leaves of Zong31, OE-1$^{ZmGLK36\text{-}Qi319}$, OE-2$^{ZmGLK36\text{-}Qi319}$ and OE-3$^{ZmGLK36\text{-}Qi319}$ lines without inoculation. We identified 791 upregulated expressed genes that are mainly enriched in plant hormone signal transduction processes and biosynthesis of secondary metabolites (Fig. 3a and Extended Data Fig. 10a). Kyoto Encyclopedia of Genes and Genomes (KEGG) analysis revealed significant enrichment in alpha-linoleic acid metabolism and plant hormone signalling pathways (Fig. 3b). As alpha-linoleic acid metabolism is a prerequisite for the production of jasmonic acid (JA)[25,35], these observations suggest a link between JA metabolism and *ZmGLK36*-mediated resistance. Given that the expression of *ZmGLK36* is induced by RBSDV infection, we speculated that its target genes should also be regulated by RBSDV in a manner similar to *ZmGLK36*. We therefore used the NIL-R line to generate a *ZmGLK36*-correlated RBSDV-responsive gene set on the basis of RBSDV-treated RNA-seq analysis. Similar enrichment in plant hormone signalling and biosynthesis of secondary metabolite pathways was found (Extended Data Fig. 10b). By overlapping the differentially expressed genes (DEGs) of the RBSDV-responsive gene set, we identified 31 potential direct target genes of *ZmGLK36* (Fig. 3c). Notably, most of them were mainly enriched in the biosynthetic pathway of JA, including jasmonate *O*-methyltransferase (*ZmJMT*) and linoleate 13S-lipoxygenase8 (*ZmLOX8*) (Fig. 3c).

As *ZmJMT* and *ZmLOX8* have been previously shown to play important roles in regulating JA signalling[36,37], we went further to test whether they are direct target genes of *ZmGLK36*. RT–qPCR assay showed that expression of *ZmJMT* and *ZmLOX8* was upregulated in the *ZmGLK36*-overexpressing plants but downregulated in the *Zmglk36* knockout plants (Extended Data Fig. 10c,d). In addition, expression of *ZmJMT* and *ZmLOX8* also displayed an RBSDV-responsive pattern similar to *ZmGLK36* in the NIL-R and NIL-S lines (Extended Data Fig. 10e,f). Y1H and transient expression assays showed that ZmGLK36 could directly bind to the promoters of *ZmJMT* and *ZmLOX8* and activate their expression (Fig. 3d,e and Extended Data Fig. 10g). Furthermore, we expressed and purified recombinant His-ZmGLK36 fusion protein (Extended Data Fig. 10h,i) and used it for EMSA assay. The results demonstrated that ZmGLK36 could markedly reduce migration of the *ZmJMT* probe, supporting direct binding of ZmGLK36 to the *ZmJMT* promoter (Fig. 3f). To verify a role of *ZmJMT* in RBSDV resistance, we isolated a *Zmjmt* mutant line from the maize EMS-mutant library[38]. RT–qPCR assay showed that the expression of *Zmjmt* was reduced by approximately half in the mutant compared to the B73 wild-type plants (Extended Data Fig. 10j). Inoculation assay showed that the *Zmjmt* mutants exhibited greater susceptibility and accumulated more RBSDV-S10 content than the *Zmglk36* knockout plants (Fig. 3g–l and Extended Data Fig. 10k,l). These results together suggest that *ZmGLK36* confers resistance to RBSDV by directly activating the expression of *ZmJMT* and *ZmLOX8*, thus increasing JA biosynthesis.

To verify the above notion, we determined JA content in various transgenic overexpression and knockout plants. The results showed that JA content was significantly higher in the ZmGLK36-overexpressing plants, but lower in the KO-1^{ZmGLK36} and KO-2^{ZmGLK36} plants compared with Zong31 (Fig. 3j). Consistently, the content of JA was significantly increased in NIL-R, but decreased in NIL-S, after inoculation with RBSDV (Fig. 3k). In addition, the JA content was significantly lower in the ZmDBF2-overexpressing plants, but higher in the KO-1^{ZmDBF2} plants compared with Zong31 (Extended Data Fig. 10m). The content of JA

Fig. 3 | ZmGLK36 promotes JA synthesis by activating *ZmJMT* expression. **a**, Venn diagram of upregulated DEGs between NIL-R (under artificial inoculation of RBSDV) and *ZmGLK36* transgenic overexpression plants. The number in each circle represents the number of upregulated genes. **b**, KEGG analysis of metabolomics-seq of Zong31 and the transgenic overexpression lines. Red represents major enrichment pathways. **c**, A heat map of the relative expression of overlapping of the DEGs of the RBSDV-responsive gene set in **a**. The colour key (orange to red) represents gene expression as fold change. For each gene, the lowest fragments per kilobase million value was set to 1.00. **d**, Y1H assay shows that ZmGLK36 binds to the promoter of *ZmJMT* and *ZmLOX8* in vitro. **e**, Transient transcriptional activity assay in maize protoplasts shows that ZmGLK36 activates *LUC* reporter gene driven by the promoters of *ZmJMT* derived from Qi319 and Ye478. p*ZmJMT*-LUC vectors themselves were used as the negative controls (without co-transfection with ZmGLK36). Values are means ± s.e.m (n = 5 repeats). **f**, EMSA shows that TRX-His-ZmGLK36 recombinant protein could bind to the putative GATTC-box in the *ZmJMT* promoter. Biotin-labelled probes and mutant probes are indicated in the bottom panel. Blue represents the binding motif and red represents the corresponding mutant sequence. TRX and His recombinant proteins without ZmGLK36 were used as negative controls. **g**, Phenotype of B73 and *Zmjmt* mutant. Scale bar, 30 cm. **h**, DSI values of B73 and *Zmjmt* mutant plants at the silking stage. Data are means ± s.e.m. from 3 biological replicates (n = 34 plants per replicate). **i**, Relative expression of RBSDV-S10 mRNA in B73 and *Zmjmt* mutant plants at the silking stage. Values are means ± s.e.m. from 3 biological replicates (n = 5 plants per replicate). **j**–**l**, Determination of JA content in Zong31, transgenic overexpression, knockout plants, B73, NIL-S and NIL-R, and *Zmjmt* mutant. JA content in NIL-S and NIL-R were measured by inoculation with RBSDV at 12 dpi. Values are means ± s.e.m from 3 biological replicates (n = 5 plants per replicate). **m**, RT–qPCR analysis of virus accumulation of S10 in RBSDV-infected maize leaves pretreated with MeJA. Data are means ± s.e.m. from 3 biological replicates (n = 5 plants per replicate). Exact P values are shown; two-sided Student's t-test.

https://doi.org/10.1038/s41477-023-01514-w

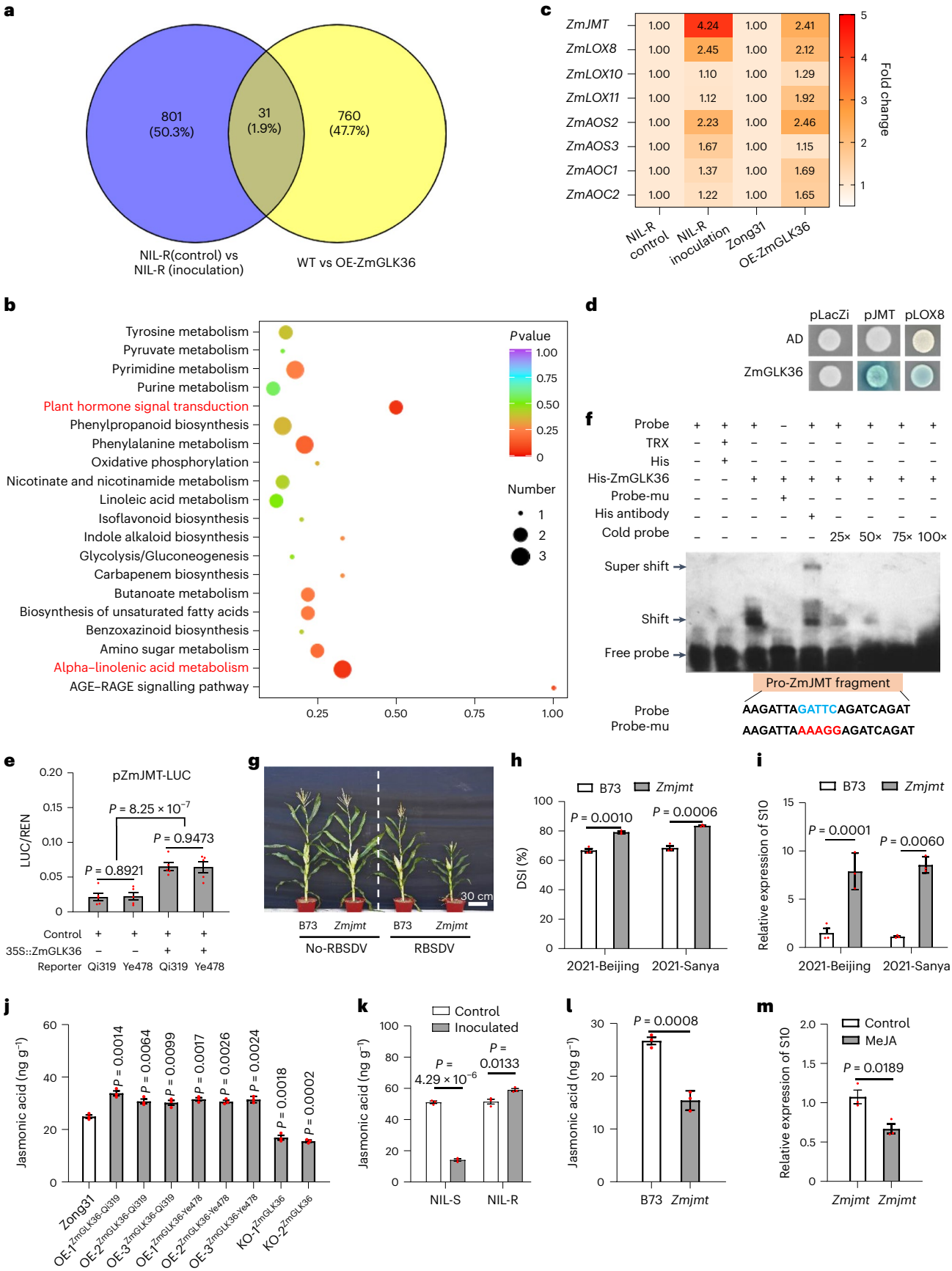

https://doi.org/10.1038/s41477-023-01514-w

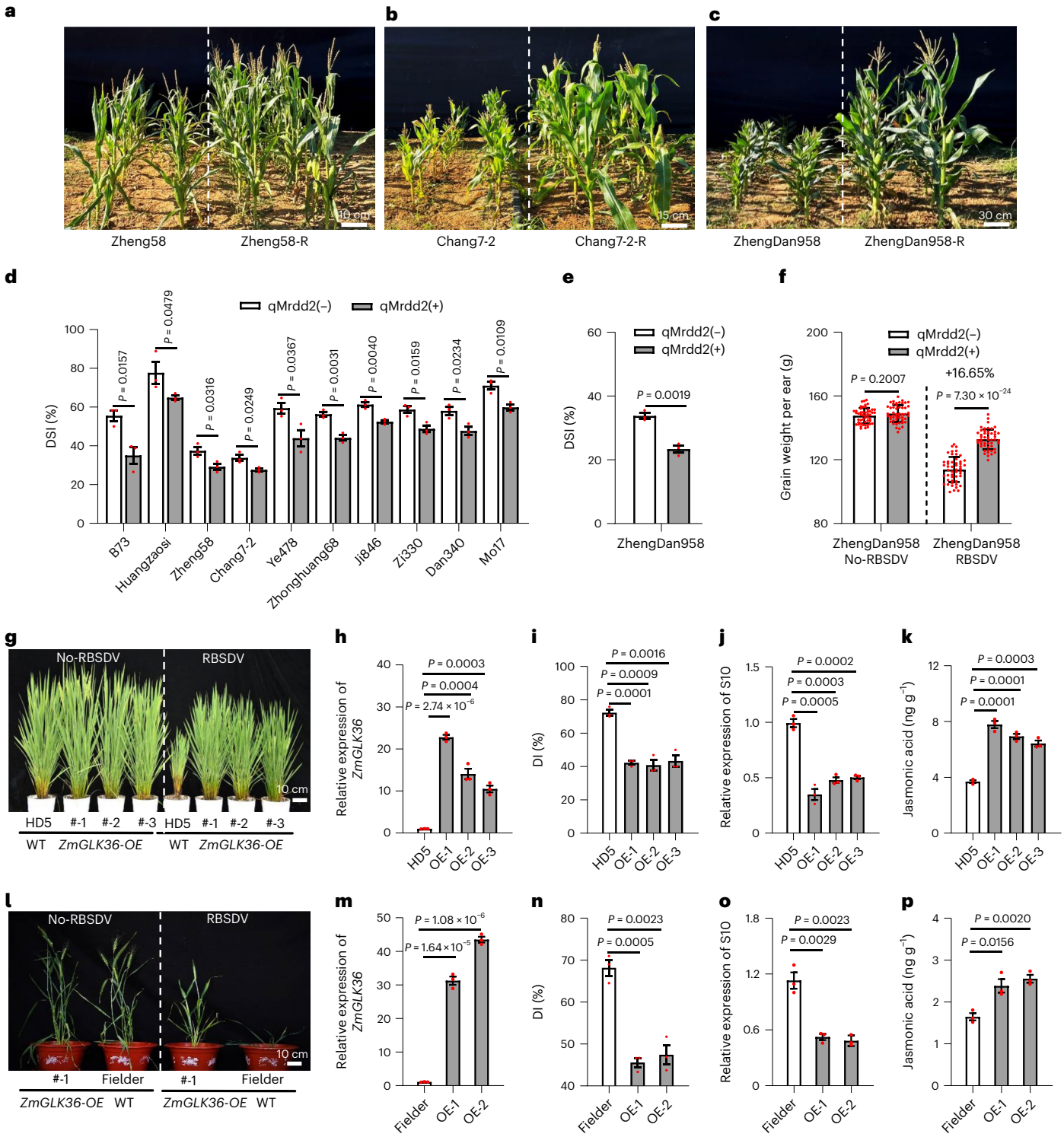

Fig. 4 | *ZmGLK36* confers broad resistance to RBSDV in maize, rice and wheat. **a**–**c**, MRDD phenotype of the improved lines (named Chang7-2-R, Zheng58-R and ZhengDan958-R) and the original Chang7-2, Zheng58 and ZhengDan958 lines growing under artificial inoculation with RBSDV. **d**,**e**, Statistical analysis of the improved lines and original lines under artificial inoculation with RBSDV at Sanya. Data are means ± s.e.m. from 3 biological replicates (n = 45 plants per replicate). **f**, Grain weight per ear of the improved hybrids and original hybrids with or without RBSDV inoculation. Data are means ± s.e.m. (n = 50 plants). **g**,**l**, Phenotypes of wild type (WT) rice and wheat, transgenic rice and wheat plants grown in Beijing. **i**,**n**, DI values of WT rice and wheat, transgenic rice and wheat plants under artificial inoculation with RBSDV at anthesis in Beijing. Data are means ± s.e.m. (n = 3 biologically independent samples). **j**,**o**, Relative expression of *RBSDV-S10* mRNA in WT rice, transgenic rice and wheat plants under artificial inoculation with RBSDV at anthesis. Data are means ± s.e.m. from 3 biological replicates (n = 5 plants per replicate). **k**,**p**, Determination of JA content in WT rice, transgenic rice and wheat plants at anthesis. Data are means ± s.e.m. from 3 biological replicates (n = 5 plants per replicate). Exact P values are shown; two-sided Student's t-test.

https://doi.org/10.1038/s41477-023-01514-w

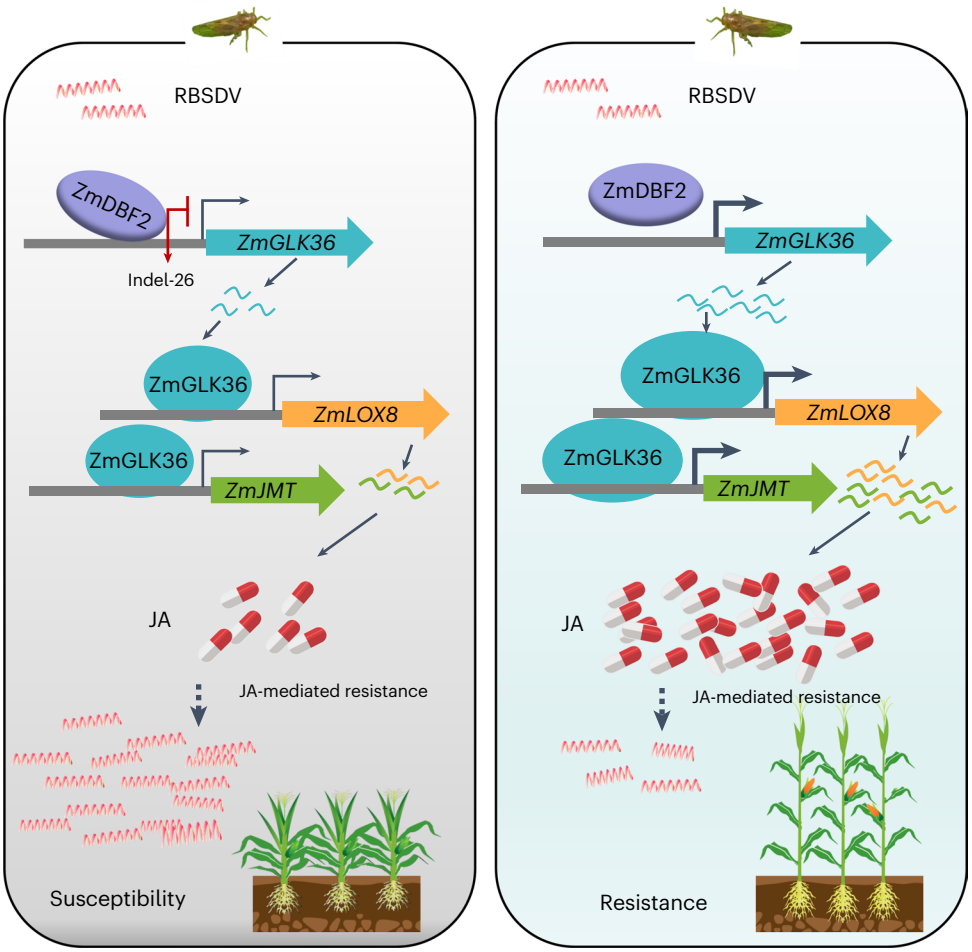

Fig. 5 | Model depicting *ZmGLK36*-mediated resistance to rough dwarf disease. In the resistant inbred lines, the expression of *ZmGLK36* was rapidly induced by RBSDV, which subsequently promotes resistance to RBSDV by enhancing JA biosynthesis and JA-mediated defence response. However, in the susceptible inbred lines, ZmDBF2 directly binds to the 26-bp indel in the *ZmGLK36* 5′ UTR and represses *ZmGLK36* expression, resulting in susceptibility to RBSDV.

was also significantly decreased in the *Zmjmt* mutants compared with B73 (Fig. 3l). Moreover, pre-application of exogenous methyl jasmonate (MeJA) could partially restore the viral resistance phenotype for the *Zmjmt* mutant (Fig. 3m and Extended Data Fig. 10n). Together, these results suggest that *ZmGLK36* confers resistance to RBSDV by promoting JA biosynthesis and JA-mediated defence response in response to RBSDV infection.

Potential application of *ZmGLK36* in crop breeding

To explore natural variation in *ZmGLK36* in maize accessions, we used the functional marker indel-26 to screen 160 American maize inbred lines (Supplementary Table 3) and 226 temperate maize inbred lines (Supplementary Table 2). We found that only 6 (3.75%) of 160 American germplasm and only 11 (4.86%) of 226 temperate maize germplasm contain the $ZmGLK36^{Qi319}$ allele (RBSDV-resistant), indicating that $ZmGLK36^{Qi319}$ is a rare allele that has not been widely utilized in modern maize breeding for resistance to RBSDV. To test the utility of $ZmGLK36^{Qi319}$ in breeding, we introgressed the $ZmGLK36^{Qi319}$ allele into 10 elite inbred lines, including Zheng58 and Chang7-2, the parental lines of the single-cross hybrid ZhengDan958 (Zheng58 × Chang7-2, an elite maize hybrid widely planted in China) by using multi-generation backcrossing and marker-assisted selection. Field tests showed that the 10 improved inbred lines and 1 hybrid all exhibited enhanced resistance to RBSDV than their respective control plants under natural and artificial inoculation of RBSDV at Jining and Sanya, respectively (Fig. 4a–e and Supplementary Fig. 1a). Moreover, the improved ZhengDan958 hybrid carrying *qMrdd2* had higher grain yield per ear (16.65%) than the original hybrid under artificial inoculation conditions (Fig. 4f). No apparent negative effects were observed on yield and other major agronomic traits under non-pathogenic stress conditions (Fig. 4f and Supplementary Fig. 1b–k).

RBSDV can also infect rice and wheat and cause heavy yield loss[22,39]. To test whether *ZmGLK36* can confer resistance to RBSDV in rice and wheat, we introduced the coding sequence of *ZmGLK36* driven by the maize ubiquitin promoter into the susceptible rice cultivar Huaidao5 (HD5) and the wheat cultivar Fielder. Three independent overexpression lines (OE-1, OE-2 and OE-3) (Fig. 4g) of rice and two independent overexpression lines (OE-1 and OE-2) (Fig. 4l) of wheat were generated and used for evaluation. RT–qPCR results showed that expression of *ZmGLK36* was increased by ~10 to 40 times in the rice and wheat overexpression lines compared with their controls (Fig. 4h,m). At 50 d after artificial inoculation with RBSDV in 2021 in Beijing, disease incidence (DI) and expression of *RBSDV-S10* of the rice OE-1, OE-2 and OE-3 lines was much lower (42.65%, 40.62% and 43.65%, respectively) than that of HD5 (72.68%) (Fig. 4i,j). Similarly, at 45 d after artificial inoculation with RBSDV in 2021 in Beijing, DI and expression of *RBSDV-S10* of the wheat OE-1 and OE-2 lines was also significantly lower (45.37% and 47.13%, respectively) than that of Fielder (68.54%) (Fig. 4n,o). Measurement of JA content showed that all the transgenic overexpressing rice and wheat plants had significantly higher JA contents than their respective

recipient backgrounds (Fig. 4k,p). These results indicate that *ZmGLK36* has broad application in breeding RBSDV-resistant cereal crops.

Discussion

MRDD is economically impactful because of its effects on the production of all major cereal crops, including rice, maize, wheat and barley[4,12,18,22]. Despite its importance, only two genes conferring RBSDV resistance have been cloned so far: *OsGLK1* and *OsAP47* from rice and *ZmGDIα-hel* from maize[20–22]. In addition, the molecular mechanisms of RBSDV resistance remain poorly understood. It was shown that reduced expression of *OsAP47* or increased expression of *OsGLK1* confers RBSDV resistance in rice and that the resistant *ZmGDIα-hel* allele weakens its binding with the viral P7-1 protein to impair virus replication[20–22]. In this study, we report the successful cloning of *qMrdd2* (encoding ZmGLK36) and elucidation of its molecular mechanism of conferring resistance to RBSDV, that is, via enhancing JA biosynthesis in response to RBSDV infection (Figs. 1, 3 and 5). Thus, our results reveal a novel mechanism of RBSDV resistance in which resistant maize cultivars suppress virus replication by activating JA biosynthesis and response. Our results are also consistent with and echo earlier studies showing that JA plays a critical role in defence against RBSDV, SRBSDV and other plant pathogens[23,31,35,40,41].

Notably, we identify a 26-bp indel located in the *ZmGLK36* 5′ UTR that contributes to differential expression and resistance to RBSDV in maize inbred lines (Figs. 1j–l and 2a–e, and Extended Data Figs. 7b,c and 8a–d). In addition, we identify ZmDBF2 (an AP2/EREBP family transcription factor) and ZmbHLH74 as two upstream regulators of *ZmGLK36* expression. We show that both ZmDBF2 and ZmbHLH74 could directly bind to the 26-bp fragment present in susceptible inbred lines, and they act to repress and activate *ZmGLK36* expression, respectively (Fig. 5 and Extended Data Fig. 8f). RT–qPCR assay showed that the expression of both *ZmDBF2* and *ZmbHLH74* could be induced by RBSDV inoculation in both NIL-R and NIL-S (Extended Data Fig. 8g,h). As $ZmGLK36^{Qi319}$ (the resistant allele), but not $ZmGLK36^{Ye478}$ (the susceptible allele), could be induced by RBSDV (Fig. 1c), we focused on the repressive role of ZmDBF2 on *ZmGLK36* in this study. We have accumulated several lines of evidence supporting a repressive role of ZmDBF2 on *ZmGLK36* expression and that this repression is dependent on the 26-bp indel present in the susceptible inbred lines. First, transient expression assay in maize protoplasts showed that ZmDBF2 exhibited significantly stronger repression on $pZmGLK36^{Ye478}$ than on $pZmGLK36^{Qi319}$ (Fig. 2g). Second, EMSA results showed that MBP-ZmDBF2 fusion protein could effectively slow down migration of the wild-type probe containing the TCTCGCT motif, but not the mutant probe in which the TCTCGCT motif was mutated into TTTTAAA (Fig. 2h). Third, RT–qPCR assay showed that expression of *ZmGLK36* was downregulated in the *ZmDBF2*-overexpressing plants, but upregulated in the *Zmdbf2* knockout plants (Extended Data Fig. 8m). It will be interesting to investigate how ZmDBF2 and ZmbHLH74 act coordinatedly to regulate *ZmGLK36* expression and RBSDV resistance in future studies.

Our population genetics study showed that the resistant allele of *ZmGLK36* (Hap 1, $ZmGLK36^{Qi319}$ type) is a rare allele that has not been extensively utilized in modern maize breeding (Supplementary Tables 2 and 3). We developed a functional marker on the basis of the 26-bp indel causal variation of *ZmGLK36* and through repeated backcrossing and molecular marker-assisted selection, we developed ten elite inbred lines harbour the resistant $ZmGLK36^{Qi319}$ allele. Field testing showed that the improved inbred lines and hybrids (for example, improved ZhengDan958) exhibited much-enhanced resistance to RBSDV and higher yield potential than their respective controls (Fig. 4a–e and Supplementary Fig. 1a). Importantly, no apparent negative effects were observed for other major agronomic traits under non-pathogenic stress conditions (Supplementary Fig. 1b–k). These observations demonstrate the great potential of *ZmGLK36* in future breeding of RBSDV-resistant maize cultivars. Nevertheless, it is worth pointing out that the phenotypic effect of *qMrdd2* (explaining 8.64% to 11.02% of the total phenotypic variance) is less than that of *qMrdd8* (encoding *RabGDIα*, explaining 24.2% of the phenotypic variance)[20,22]. Thus, it will be worth stacking up both *qMrdd2* and *qMrdd8* to achieve higher resistance to RBSDV in maize production.

It is also worth pointing out that the previously reported RBSDV resistance genes *OsGLK1*, *OsAP47* and *RabGDIα* have only been functionally verified in rice and maize, respectively[20–22], and it is unknown whether these genes could be leveraged to breed MRDD-resistant cultivars of other crops. Here we show that transgenic rice and wheat plants overexpressing *ZmGLK36* exhibit much-enhanced resistance to RBSDV (Fig. 4g–p), suggesting that *ZmGLK36* probably plays a conserved role in mediating defence response against RBSDV and related viruses (such as MRDV and SRBSDV), and therefore has broad utility in breeding cereal crops resistant to RBSDV and related viruses. Future work is aimed to test such a possibility.

Methods

Plant materials

The resistant line Qi319 was derived from the US hybrid 78599. The susceptible line Ye478 was derived from the cross U8112 × 5003 and developed into an elite inbred line that has been used widely in maize breeding programmes in China. The recombinant inbred line (RIL) population was derived from a cross between Ye478 (susceptible) and Qi319 (resistant)[32]. A pair of NILs called NIL-S and NIL-R was generated by repeated backcrossing of the resistant inbred line Qi319 to the susceptible inbred line Ye478 with marker-assisted selection[12]. Maize inbred lines (226) have been genotyped with 41,101 SNPs using the maize SNP50 BeadChip technique[42]. Elite inbred lines (160) obtained from the US National Plant Germplasm System were used for assessing the RBSDV resistance phenotype on the basis of the 26-bp indel functional marker. Transgenic plants were generated in Beijing Origen Guofeng Biotechnology using the susceptible maize inbred line Zong31 as the recipient. The *Zmjmt* mutant (in the B73 background) was isolated from an EMS-mutagenized maize library[38]. The *Zmjmt* mutant was backcrossed once with the wild-type B73 and then selfed twice to reduce the background mutations. The rice cultivar Huaidao5 and wheat cultivar Fielder were used as the transgenic recipients. Transgenic rice and wheat plants were grown in isolated paddy fields during natural growing seasons at the Chinese Academy of Agricultural Sciences (Beijing, China).

Artificial inoculation of RBSDV and phenotyping

Maize, rice and wheat were artificially inoculated with RBSDV at the 3-leaf (V3) stage of seedlings with viruliferous SBPH, while the control materials were inoculated with virus-free SBPH. After 48 h of inoculation, SBPH were removed to avoid over infestation and the plants were then transplanted into the field. Each plant was investigated for MRDD symptoms at the silking stage (for maize) and anthesis of rice and wheat. Naturally inoculated maize were planted around 10–20 May at Jining in Shandong Province (35.38° N, 116.59° E). The artificially inoculated maize materials were planted at Sanya in Hainan Province (18.25° N, 109.5° E) or Beijing (40.13° N, 116.65° E). MRDD symptoms were scored on a scale from 0 to 4, in which plants scored 0 were highly resistant and those scored 4 were highly susceptible to MRDD. DSI was used to represent MRDD severity and defined as follows[12]: DSI (%) = Σ (disease rating score × number of plants with each score)/(maximum disease rating score × total number of plants rated in the line) × 100.

Initial Qi319 and Ye478 genome assembly

De novo assembly and annotation of the Ye478 genome was reported in ref. 43. For de novo assembly and annotation of the Qi319 genome, genomic DNA was extracted from V3 seedlings using the DNeasy plant mini kit (Qiagen). A 15-kb library was constructed and sequenced using the Pacific Bioscience Sequel II platform (Annoroad Gene Technology).

CCS reads (39.66 Gb) with an N50 size of 16.01 kb were generated using the ccs software v.3.0.0 (https://github.com/, pacific biosciences/unanimity/,–min-passes 3–min-length 10000–max-length 1000000–min-rq 0.99). For high-throughput chromosome conformation capture (Hi-C), the libraries were controlled for quality and sequenced on an Illumina Hiseq NovaSeq platform. DpnII was used as the restriction enzyme in chromatin digestion. The library was constructed using an Illumina TruSeq DNA sample prep kit and sequenced using Illumina Hiseq Xten with 2× 150-bp reads. For RNA-seq, samples of leaf, spikelet, root, embryo, endosperm, filament, stem and tassel were collected separately at the corn milk maturity stage. Total RNA was isolated using the RNAprep Pure plant kit (TIANGEN). RNA-seq library construction was performed following a previously published method and sequenced on the NovaSeq platform[43].

A contig genome was assembled from hifi reads using the software hifiasm with default parameters. Then the contigs were anchored onto chromosomes using Hi-C reads. Hi-C reads were aligned to contigs using HICUP (v.0.7.3), yielding an alignment BAM file. Contigs were then clustered using the ALLHiC algorithm. Finally, the assembled genome was manually corrected with Juicebox (v.1.11.08). Benchmarking universal single-copy orthologues (BUSCO) and LTR assembly index (LAI) were used to determine completeness on the basis of the embryophyte plant database and full-length long terminal repeats retrotransposon, respectively.

The annotation pipeline for prediction of repeat elements included de novo and homology-based approaches. For homologue evidence, alignment searches were undertaken against the RepBase database (http://www.girinst.org/repbase) and then predicted using Repeat Protein Mask (http://www.repeatmasker.org/). For de novo annotation, LTR_FINDER, PILER, RepeatScout (http://www.repeatmasker.org/) and Repeat-Modeler (v.2.0.3) (http://www.repeatmasker.org/RepeatModeler.html) were used to construct a de novo library, then annotation was carried out with Repeat masker (v.4.1.2) (http://repeatmasker.org/).

ZmGLK36-based association analysis

According to the sequences of the B73_V4 reference genome, 10 pairs of primers were designed (Prime 5.0) to amplify *ZmGLK36* from 97 maize inbred lines (Supplementary Table 2). The sequences were assembled using DNAMAN and aligned with MEGA 5.0. The DNA variations of SNPs and indels were identified among these genotypes and their association with the phenotype and pairwise linkage disequilibrium (LD) were calculated using Tassel 5.0 (refs. 44,45).

Histological and promoter activity assays

NIL-S and NIL-R were artificially inoculated with RBSDV at the V3 stage of maize seedlings. Around the silk spitting period, stalks were selected from the middle of the 8th internode of NIL-R and NIL-S. The stalks were subsequently cut into fine pieces and submerged into 2.5% glutaraldehyde in phosphate buffer (pH 7.2) for more than 4 h at 4 °C. Samples were post-fixed in PBS buffer for 2 h and washed three times with PBS. The fixed samples were dehydrated through a graded series of ethanol for ~30 min at each step. Thereafter, the samples were dried and coated with conductive materials and examined under an S-3400N Hitachi scanning electron microscope for photographing (Hitachi).

The GUS transgenic plants were inoculated at the V3 stage of maize seedlings and inoculation was performed as described above. The inoculated maize leaves and control materials were immersed in the GUS staining solution and held at 25–37 °C for 1 h to overnight. Subsequently, they were transferred to 70% ethanol and decolorized 2–3 times until the negative control material was white. The GUS staining kit was obtained from Beijing Huayueyang Biotechnology.

RNA extraction and expression analysis

For detection of expression in response to RBSDV infection, the plants were inoculated at the V3 stage of maize seedlings as described above. NIL-R and NIL-S were inoculated with poisonous SBPH, and leaves were sampled at 1.5, 6, 12, 24 and 48 dpi. The control samples were inoculated with non-toxic SBPH and sampled at the same timepoints. Leaf tissues of the GUS transgenic plants, RILs and maize inbred lines of different haplotypes were collected at 12 dpi with poisonous SBPH.

Total RNA was extracted using the EasyPure plant RNA kit (TransGen Biotech). The RNAs were quantified using a NanoDrop ND-1000 spectrophotometer (NanoDrop Technologies) and 1.0 μg of total RNAs was reversed transcribed using M-MLV reverse transcriptase (Promega, M1701). Quantitative PCR was implemented using the SYBR Premix Ex *Taq* II (Takara) on an ABI 7500 real-time detection system (Applied Biosystems) and three independent RNA samples were prepared for each biological replicate. *ZmGAPDH* was used as the internal reference. The relevant primers for RT–qPCR are listed in Supplementary Table 6. The relative transcript level was calculated using the $2^{-\Delta\Delta Ct}$ method[46].

Subcellular localization and messenger (m)RNA in situ hybridization

To determine the subcellular localization of the ZmGLK36 protein, we amplified the full-length CDS of *ZmGLK36* without the stop codon from Qi319 and Ye478 and cloned them into the pAN580-GFP vector (*35S::ZmGLK36::GFP*). The CDS of *ZmGLK36* with the stop codon was also amplified and cloned into the pAN580-YFP vector to generate the *35S::YFP::ZmGLK36*. TF3 (ref. 47) was used as a nuclear marker. The fusion plasmid and nuclear marker were co-transfected into maize protoplasts using the polyethylene glycol mediated transformation method as described previously[48]. After culturing at 25 °C for 12–18 h in the dark, the fluorescence signals were captured using a confocal laser-scanning microscope (TCS SP5, Leica). Primers used for amplification are shown in Supplementary Table 6.

For preparing the probe for in situ hybridization, a conserved sequence was amplified from the *ZmGLK36* coding region and cloned into a pGEM-T vector (Promega) for RNA probe preparation. DIG Northern starter kit (Roche) was used to generate the digoxigenin-labelled RNA probes. Leaves of Qi319 at the V3 stage of seedlings were fixed in RNase-free formaldehyde-acetic acid for 12 h and then dehydrated through a graded series of ethanol for ~30 min at each step. In situ hybridization experiments and immunological detection of the signals were performed as described previously[49]. Microscopic examination and photographing were conducted under bright field using a Leica DMR microscope (Leica DM5000B) and a camera fitted with a Micro Color CCD (Apogee Instruments). The primer sequences are shown in Supplementary Table 6.

Constructs for genetic transformation

For *ZmGLK36*, we constructed a complementary vector, two overexpression vectors and a knockout vector. For the complementary vector, a ~5-kb DNA fragment of *ZmGLK36* containing a 2-kb upstream sequence of ATG, the *ZmGLK36* genome sequence and a 400-bp downstream sequence of the 3′ UTR was amplified from Qi319 and cloned into pCAMBIA3301 (ref. 20) to generate the complementary construct. The three independent transgenic lines were named #-$1^{ZmGLK\text{-}Qi319}$, #-$2^{ZmGLK\text{-}Qi319}$ and #-$3^{ZmGLK\text{-}Qi319}$. For the overexpression construct, the full-length coding sequence of *ZmGLK36* from Qi319 and Ye478 was inserted into the CUB vector[50] under control of the maize ubiquitin promoter (UBI) to generate the *pUbi::ZmGLK36*^{Qi319} and *pUbi::ZmGLK36*^{Ye478} overexpression constructs, respectively. Six independent transgenic strains were obtained and named OE-$1^{ZmGLK36\text{-}Qi319}$, OE-$2^{ZmGLK36\text{-}Qi319}$, OE-$3^{ZmGLK36\text{-}Qi319}$, OE-$1^{ZmGLK36\text{-}Ye478}$, OE-$2^{ZmGLK36\text{-}Ye478}$ and OE-$3^{ZmGLK36\text{-}Ye478}$ using Zong31 as the transgenic recipient materials. For the CRISPR/Cas9 construct, single-guide (sgRNAs) or two-guide RNAs containing 23-bp targeting sequences were designed on the basis of the Zong31 and B73 reference genome sequences (named: KO-$1^{ZmGLK36}$ and KO-$2^{ZmGLK36}$ in Zong31; KO-26 in B73) using the CRISPR-P web tool

(http://cbi.hzau.edu.cn/crispr/). sgRNA arrays were cloned into the pCXB053 binary vector[51] following manufacturer-suggested protocols. For *ZmDBF2*, the full-length coding sequence of *ZmDBF2* from Ye478 was cloned into the CUB vector. Three overexpression lines were obtained and named OE-1^{ZmDBF2}, OE-2^{ZmDBF2} and OE-3^{ZmDBF2}. For CRISPR knockout of *ZmDBF2*, double-guide RNAs or sgRNAs were designed on the basis of the Zong31 reference genome sequence (named KO-1^{ZmDBF2} in Zong31) using the CRISPR-P web tool (http://cbi.hzau.edu.cn/crispr/). sgRNA arrays were cloned into the pCXB053 binary vector following manufacturer-suggested protocols[51].

For testing the role of the 26-bp indel in the 5′ UTR of *ZmGLK36* in response to RBSDV, we first isolated a ~1,500-bp DNA fragment upstream of the *ZmGLK36* coding region from Qi319 and artificially synthesized a 1,526-bp promoter fragment containing the 26-bp indel, both of which were introduced into the pCAMIBIA1305 vector upstream of the GUS reporter gene to generate the *pZmGLK36*^{Qi319}::GUS and *pZmGLK36*$^{Qi319+26}$::GUS reporter constructs, respectively. Because the pCAMIBIA1305 vector cannot be used to transform maize, the completed promoter and GUS fusion vector sequences were subsequently cloned into the pTF101.1 vector[52] and used to transform Zong31. All resulting vectors were confirmed by sequencing, and *Agrobacterium*-mediated transformation was used to generate transgenic maize plants[53]. All transgenic seeds were created by Beijing Origin State Harvest Biotechnology. For the CRISPR/Cas9 lines, the target sites of the genomic fragment and Cas9 gene were detected from the T_0–T_2 plants using PCR and basta resistance. The PCR products were separated on agarose gels and cloned into the pEASY-Blunt Simple Cloning vector (TransGen Biotech) for sequencing analysis. The homozygous mutant lines without Cas9 were selected and selfed for seed propagation. Primer sequences used in constructing various transgenic vectors and RT–qPCR are listed in Supplementary Table 6.

The transgenic complementary (*ZmGLK36*), overexpression (*ZmGLK36* and *ZmDBF2*) and knockout (*ZmGLK36* and *ZmDBF2*) plants were planted from T_1 to T_3 to obtain homozygous lines. Subsequently, T_3 homozygous plants were used for inoculation and phenotypic assays as described above.

Metabolomics and RNA-seq analyses

For the metabolomics-seq, maize inbred line Zong31 and the *ZmGLK36* overexpression plants were planted in Beijing in 2021. The top fresh leaves of maize were taken at the V3 stage. The samples were subjected to RT–qPCR to detect the expression of *ZmGLK36* to ensure the accuracy and reliability of the samples. Subsequently, triplicate biological samples were placed in a lyophiliser (Scientz-100F) for vacuum freeze-drying and ground (30 Hz, 1.5 min) into powder using a grinder (MM 400, Retsch). Then, 100 mg of the powder was dissolved in 1.2 ml of 70% methanol extract, vortexed 6 times (30 s every 30 min) and placed in a 4 °C refrigerator overnight. After centrifugation (1,000 × *g*, 10 min), the supernatant was aspirated, filtered through a microporous membrane (0.22 μm pore size) and stored in a sample vial for UPLC–MS/MS analysis. The data acquisition instrument system mainly included an ultra-performance liquid chromatography (UPLC) (SHIMADZU Nexera X2, https://www.shimadzu.com.cn/) and tandem mass spectrometry (MS/MS) (Applied Biosystems 4500 Q-TRAP, http://www.appliedbiosystems.com.cn/) system. The analysis process was completed by Wuhan Metware Biotechnology. For RNA-seq analysis, the maize inbred line Zong31, the *ZmGLK36* overexpression plants, NIL-R and NIL-R (inoculated with viruliferous SBPH) were sequenced on an Illumina Hiseq 4000 platform by Beijing Allwegene and paired-end 150-bp reads were generated. The obtained raw data were first mapped to the B73_V4 reference genome, then Picard tools v.1.41 and samtools v.0.1.18 were used to sort and remove the duplicated reads. The bam alignment results were merged for each sample, then HTSeq v.0.5.4 p3 was used to count the read numbers mapped to each gene. DESeq functions were used to identify the differentially expressed genes ($P < 0.05$ and fold change ≥1). Gene ontology enrichment analysis of the DEGs was implemented by the GOseq R packages based on Wallenius non-central hyper-geometric distribution, which can adjust for gene length bias in DEGs. The KOBAS software was used to test the statistical enrichment of differential expression genes in KEGG pathways[54].

Y1H and Y2H assays

For the Y1H assay, the full-length CDS of *ZmGLK36*, *ZmDBF2*, *ZmP1* and *ZmbHLH74* with the stop codon from Ye478 were amplified and cloned into the pB42AD vector to generate the *pB42AD-ZmGLK36*, *pB42AD-ZmDBF2*, *pB42AD-ZmP1* and *pB42AD-ZmbHLH74* constructs, respectively. The 26-bp indel containing the binding sites of ZmDBF2, ZmP1, ZmbHLH74 and GATTC-box of ZmGLK36 from the *ZmJMT* and *ZmLOX8* promoter was amplified and cloned into the *pLacZ* reporter vector[51] to generate *26-LacZ*, *pJMT-LacZ* and *pLOX8-LacZ*. Subsequently, various plasmid combinations (*pB42AD-ZmGLK36* + *pJMT-LacZ*, *pB42AD-ZmGLK36* + *pLOX8-LacZ*, *pB42AD-ZmDBF2* + *26-LacZ*, *pB42AD-ZmP1* + *26-LacZ*, *pB42AD-ZmbHLH74* + *26-LacZ*) were respectively co-transformed into the EGY48 yeast cells (Clontech). The empty vector pB42AD and the *pLacZ* reporter vectors containing the promoter of *ZmGLK36*, *ZmJMT* and *ZmLOX8* were co-transformed into the EGY48 yeast cells as controls.

For the Y2H assay, the coding sequences of ZmGLK36 and 13 proteins of RBSDV were cloned into pGBKT7 and pGADT7 to generate the *pGBKT7-ZmGLK36*, *pGADT7-S1*, *pGADT7-S2*, *pGADT7-S3*, *pGADT7-S4*, *pGADT7-S5-1*, *pGADT7-S5-2*, *pGADT7-S6*, *pGADT7-S7-1*, *pGADT7-S7-2*, *pGADT7-S8*, *pGADT7-S9-1*, *pGADT7-S9-2* and *pGADT7-S10* constructs, respectively. Subsequently, Y2H gold competent cells (Clontech) were co-transformed with *BD-ZmGLK36* and different *pGADT7-S1* to *pGADT7-S10*. *pGBKT7-Lam* and *pGADT7-T*, *pGBKT7-53* and *pGADT7-T* were co-transfected into yeast Y2H competent cells as the positive and negative controls, respectively. All the yeast transformants were grown on an SD/-Leu/-Trp medium and then transferred to an SD/-Leu/-Trp/-His/-Ade/-X-α-gal medium for selection and interaction test. Yeast transformation was performed following the Yeast Protocols Handbook (Clontech). The primers are listed in Supplementary Table 6.

EMSA

For protein expression and purification, the full-length CDS of *ZmGLK36* and *ZmDBF2* were amplified and cloned into the pET-32a and pMAL-c5x vector to generate *His-ZmGLK36* and *MBP-ZmDBF2* constructs, respectively. The two fusion constructs were each introduced into *E. coli* Rosetta cells (TransGen Biotech). Expression of the fusion protein His-ZmGLK36 and MBP-ZmDBF2 were induced by isopropyl-β-D-thiogalactopyranoside and purified using IDA-nickel beads (Kangma Biotechnology, PROTN_HMBN1V00005) according to manufacturer instructions. Oligonucleotide probes were synthesized and labelled with biotin at the 5′ end (Invitrogen). Western blot was conducted using anti-His antibody and anti-MBP antibody (Sigma-Aldrich) at a 1:1,000 dilution as described previously[33]. EMSA was carried out using the Light Shift Chemiluminescent EMSA kit (Thermo Fisher, 20148X). The sequences of primers used in protein expression and probes used in EMSA are listed in Supplementary Table 6.

Transient expression assays in maize protoplast

To analyse the transcriptional repressive activity of ZmDBF2 protein on *ZmGLK36*, the 127-bp and 101-bp DNA fragments upstream of the *ZmGLK36* coding region were amplified from Ye478 and Qi319 and cloned into the pGreenII 0800-35S::LUC vector[55] to generate the *proZmGLK36-35S::127:LUC* and *proZmGLK36-35S::101:LUC* constructs, respectively. The pGreenII 0800-LUC vector was modified in advance in which the mini35S promoter was amplified and inserted into pGreenII 0800-LUC. The full-length CDS of *ZmDBF2* and *ZmbHLH74* were amplified from Ye478 and inserted into pAN580 to generate the *pAN580-35S::ZmDBF2* and *pAN580-35S::Zm bHLH74*

effector constructs, respectively. Approximately 1.7-kb DNA fragments upstream of *ZmJMT* and *ZmLOX8* coding regions were amplified from Qi319 and Ye478 and inserted into pGreenII 0800-LUC vector to generate the *proZmGLK36-Qi319::LUC* and *proZmGLK36-Ye478::LUC* constructs, respectively. Full-length CDS of *ZmGLK36* were amplified from Ye478 and inserted into pAN580 to generate the *pAN580-35S::ZmGLK36* effector. The transient dual-luciferase assay was performed in the maize protoplasts as described previously[48]. A Dual-Luciferase Reporter Assay System kit (Promega, E1960) was used to examine the activities of firefly luciferase (LUC) and *Renilla* luciferase (REN). LUC/REN was calculated as the relative activity. Five replicates were performed for each effector. The sequences of primers used in the transient expression assay are listed in Supplementary Table 6.

Statistics

Two-sided Student's *t*-test was used to test the significance of differences between two groups using Excel 2010. Tukey's honestly significant difference (HSD) test was performed using GraphPad Prism v.8.0.

Reporting summary

Further information on research design is available in the Nature Portfolio Reporting Summary linked to this article.

Data availability

The datasets generated and/or analysed during the current study are provided with this paper. Any additional data are available from the corresponding author. No participant identifiable information will be disclosed. Source data are provided with this paper.

Code availability

The custom codes used in this study are deposited in GitHub (https://github.com/wangtao-go/fpkm/blob/main/calRPKM.pl).

References

1. Soosaar, J. L., Burch-Smith, T. M. & Dinesh-Kumar, S. P. Mechanisms of plant resistance to viruses. *Nat. Rev. Microbiol.* **3**, 789–798 (2005).
2. Kang, B. C., Yeam, I. & Jahn, M. M. Genetics of plant virus resistance. *Annu. Rev. Phytopathol.* **43**, 581–621 (2005).
3. Achon, M. A., Serrano, L., Sabate, J. & Porta, C. Understanding the epidemiological factors that intensify the incidence of maize rough dwarf disease in Spain. *Ann. Appl. Biol.* **166**, 311–320 (2015).
4. Yang, Q., Balint-Kurti, P. & Xu, M. Quantitative disease resistance: dissection and adoption in maize. *Mol. Plant* **10**, 402–413 (2017).
5. Miao, H.-Q. et al. Efficient inoculation of rice black-streaked dwarf virus to maize using *Laodelphax striatellus* Fallen. *J. Phytopathol.* **163**, 529–535 (2015).
6. Cheng, Z. et al. Distribution and genetic diversity of southern rice black-streaked dwarf virus in China. *Virol. J.* **10**, 307 (2013).
7. Fang, S. et al. Identification of rice black-streaked dwarf fijivirus in maize with rough dwarf disease in China. *Arch. Virol.* **146**, 167–170 (2001).
8. Lenardon, S. L., March, G. J., Nome, S. F. & Ornaghi, J. A. Recent outbreak of "Mal de Rio Cuarto" virus on corn in Argentina. *Plant Dis.* **82**, 448 (1998).
9. Liu, J., Fernie, A. R. & Yan, J. The past, present, and future of maize improvement: domestication, genomics, and functional genomic routes toward crop enhancement. *Plant Commun.* **1**, 100010 (2020).
10. Liu, C. et al. Fine mapping of a quantitative trait locus conferring resistance to maize rough dwarf disease. *Theor. Appl. Genet.* **129**, 2333–2342 (2016).
11. Tao, Y. et al. Identification and fine-mapping of a QTL, qMrdd1, that confers recessive resistance to maize rough dwarf disease. *BMC Plant Biol.* **13**, 145 (2013).
12. Xu, Z. et al. Identification and fine-mapping of a novel QTL, qMrdd2, that confers resistance to maize rough dwarf disease. *Plant Dis.* **106**, 65–72 (2022).
13. Zhang, W. et al. qMrdd2, a novel quantitative resistance locus for maize rough dwarf disease. *BMC Plant Biol.* **21**, 307 (2021).
14. Wang, X. et al. Identification of QTLs for resistance to maize rough dwarf disease using two connected RIL populations in maize. *PLoS ONE* **14**, e0226700 (2019).
15. Luan, J., Wang, F., Li, Y., Zhang, B. & Zhang, J. Mapping quantitative trait loci conferring resistance to rice black-streaked virus in maize (*Zea mays* L.). *Theor. Appl. Genet.* **125**, 781–791 (2012).
16. Zhao, M. et al. Identification of genetic loci associated with rough dwarf disease resistance in maize by integrating GWAS and linkage mapping. *Plant Sci.* **315**, 111100 (2022).
17. Li, R. et al. Identification of a locus conferring dominant resistance to maize rough dwarf disease in maize. *Sci. Rep.* **8**, 3248 (2018).
18. Feng, Z. et al. Identification of new rice cultivars and resistance loci against rice black-streaked dwarf virus disease through genome-wide association study. *Rice* **12**, 49 (2019).
19. Liu, Q. et al. Genome-wide association study on resistance to rice black-streaked dwarf disease caused by rice black-streaked dwarf virus. *Plant Dis.* **105**, 607–615 (2021).
20. Liu, Q. et al. A helitron-induced RabGDIalpha variant causes quantitative recessive resistance to maize rough dwarf disease. *Nat. Commun.* **11**, 495 (2020).
21. Li, X. et al. Golden 2-like transcription factor contributes to the major QTL against rice black-streaked dwarf virus disease. *Theor. Appl. Genet.* **135**, 4233–4243 (2022).
22. Wang, Z. et al. An aspartic protease 47 causes quantitative recessive resistance to rice black-streaked dwarf virus disease and southern rice black-streaked dwarf virus disease. *New Phytol.* **233**, 2520–2533 (2022).
23. Browse, J. Jasmonate passes muster: a receptor and targets for the defense hormone. *Annu. Rev. Plant Biol.* **60**, 183–205 (2009).
24. Chen, Y. et al. Cloning of wheat keto-acyl thiolase 2B reveals a role of jasmonic acid in grain weight determination. *Nat. Commun.* **11**, 6266 (2020).
25. Gomi, K. Jasmonic acid: an essential plant hormone. *Int. J. Mol. Sci.* **21**, 1261 (2020).
26. Hickman, R. et al. Architecture and dynamics of the jasmonic acid gene regulatory network. *Plant Cell* **29**, 2086–2105 (2017).
27. Pauwels, L. et al. Mapping methyl jasmonate-mediated transcriptional reprogramming of metabolism and cell cycle progression in cultured *Arabidopsis* cells. *Proc. Natl Acad. Sci. USA* **105**, 1380–1385 (2008).
28. Truman, W., Bennett, M. H., Kubigsteltig, I., Turnbull, C. & Grant, M. *Arabidopsis* systemic immunity uses conserved defense signaling pathways and is mediated by jasmonates. *Proc. Natl Acad. Sci. USA* **104**, 1075–1080 (2007).
29. Yang, Z. et al. Jasmonate signaling enhances RNA silencing and antiviral defense in rice. *Cell Host Microbe* **28**, 89–103.e108 (2020).
30. Ruan, J. et al. Jasmonic acid signaling pathway in plants. *Int. J. Mol. Sci.* **20**, 2479 (2019).
31. Li, L. et al. A class of independently evolved transcriptional repressors in plant RNA viruses facilitates viral infection and vector feeding. *Proc. Natl Acad. Sci. USA* **118**, e2016673118 (2021).
32. Zhou, Z. et al. Genetic dissection of maize plant architecture with an ultra-high density bin map based on recombinant inbred lines. *BMC Genomics* **17**, 178 (2016).
33. Kizis, D. & Pagès, M. Maize DRE-binding proteins DBF1 and DBF2 are involved in rab17 regulation through the drought-responsive element in an ABA-dependent pathway. *Plant J.* **30**, 679–689 (2002).

34. Rhee, Y., Sekhon, R. S., Chopra, S. & Kaeppler, S. Tissue culture-induced novel epialleles of a Myb transcription factor encoded by pericarp color1 in maize. *Genetics* **186**, 843–855 (2010).
35. Lyons, R., Manners, J. M. & Kazan, K. Jasmonate biosynthesis and signaling in monocots: a comparative overview. *Plant Cell Rep.* **32**, 815–827 (2013).
36. Christensen, S. A. et al. The maize lipoxygenase, ZmLOX10, mediates green leaf volatile, jasmonate and herbivore-induced plant volatile production for defense against insect attack. *Plant J.* **74**, 59–73 (2013).
37. Stitz, M., Gase, K., Baldwin, I. T. & Gaquerel, E. Ectopic expression of AtJMT in *Nicotiana attenuata*: creating a metabolic sink has tissue-specific consequences for the jasmonate metabolic network and silences downstream gene expression. *Plant Physiol.* **157**, 341–354 (2011).
38. Lu, X. et al. Gene-indexed mutations in maize. *Mol. Plant* **11**, 496–504 (2018).
39. Zhou, T. et al. Inheritance and mechanism of resistance to rice stripe disease in cv. Zhendao 88, a Chinese rice cultivar. *J. Phytopathol.* **159**, 159–164 (2011).
40. He, L. et al. Rice black-streaked dwarf virus-encoded P5-1 regulates the ubiquitination activity of SCF E3 ligases and inhibits jasmonate signaling to benefit its infection in rice. *New Phytol.* **225**, 896–912 (2020).
41. He, Y. et al. Jasmonic acid-mediated defense suppresses brassinosteroid-mediated susceptibility to rice black-streaked dwarf virus infection in rice. *New Phytol.* **214**, 388–399 (2017).
42. Liu, C. et al. Genetic properties of 240 maize inbred lines and identity-by-descent segments revealed by high-density SNP markers. *Mol. Breed.* **35**, 146 (2015).
43. Wang, B. et al. De novo genome assembly and analyses of 12 founder inbred lines provide insights into maize heterosis. *Nat. Genet.* **55**, 312–323 (2023).
44. Bradbury, P. J. et al. TASSEL: software for association mapping of complex traits in diverse samples. *Bioinformatics* **23**, 2633–2635 (2007).
45. Zhang, Z. et al. Mixed linear model approach adapted for genome-wide association studies. *Nat. Genet.* **42**, 355–360 (2010).
46. Schmittgen, T. D. & Livak, K. J. Analyzing real-time PCR data by the comparative C(T) method. *Nat. Protoc.* **3**, 1101–1108 (2008).
47. Wang, K. et al. Wheat Elongator Subunit 4 negatively regulates freezing tolerance by regulating ethylene accumulation. *Int. J. Mol. Sci.* **23**, 7634 (2022).
48. Yoo, S. D., Cho, Y. H. & Sheen, J. *Arabidopsis* mesophyll protoplasts: a versatile cell system for transient gene expression analysis. *Nat. Protoc.* **2**, 1565–1572 (2007).
49. Wu, M. F. & Wagner, D. RNA in situ hybridization in *Arabidopsis*. *Methods Mol. Biol.* **883**, 75–86 (2012).
50. Du, Q., Wang, K., Zou, C., Xu, C. & Li, W. X. The PILNCR1-miR399 regulatory module is important for low phosphate tolerance in maize. *Plant Physiol.* **177**, 1743–1753 (2018).
51. Liu, H. J. et al. High-throughput CRISPR/Cas9 mutagenesis streamlines trait gene identification in maize. *Plant Cell* **32**, 1397–1413 (2020).
52. Paz, M. M. et al. Assessment of conditions affecting *Agrobacterium*-mediated soybean transformation using the cotyledonary node explant. *Euphytica* **136**, 167–179 (2004).
53. Ishida, Y., Hiei, Y. & Komari, T. *Agrobacterium*-mediated transformation of maize. *Nat. Protoc.* **2**, 1614–1621 (2007).
54. Bu, D. et al. KOBAS-i: intelligent prioritization and exploratory visualization of biological functions for gene enrichment analysis. *Nucleic Acids Res.* **49**, 317–325 (2021).
55. Liu, Y. et al. DWARF53 interacts with transcription factors UB2/UB3/TSH4 to regulate maize tillering and tassel branching. *Plant Physiol.* **187**, 947–962 (2021).

Acknowledgements

This work was supported by the National Key Research and Development Program of China (2022YFD1201802 and 2020YFE0202300), the National Natural Science Foundation of China (31771804), the Agricultural Science and Technology Innovation Program (CAAS-ZDRW202109) and the Modern Agro-Industry Technology Research System of Maize (CARS-02-02).

Author contributions

Z.X. performed most of the experiments. Z.X., Z.Z., H.W., J.W. and X. Li designed experiments and wrote the manuscript. Z.C., Q.D. and Y.T. designed the CRISPR target and constructed the plasmid library. W.L., Y.Z. and X. Lu analysed the data. F.W., R.C. and G.L. characterized the genotypes and phenotypes of the edited lines. K.W and W.S. carried out the transformation of transgenic wheat and in part, maize. S.T., M.L., D.Z., H.Y., C.M., Z.H., Z.W. and J.H. provided 226 temperate and 160 American inbred lines of maize. Y.C., Q.M. and X.K. performed the artificial inoculation of RBSDV and field management.

Competing interests

The authors declare no competing interests.

Additional information

Extended data is available for this paper at https://doi.org/10.1038/s41477-023-01514-w.

Supplementary information The online version contains supplementary material available at https://doi.org/10.1038/s41477-023-01514-w.

Correspondence and requests for materials should be addressed to Haiyang Wang, Jianfeng Weng or Xinhai Li.

Peer review information *Nature Plants* thanks Zuhua He, Beat Keller and the other, anonymous, reviewer(s) for their contribution to the peer review of this work.

https://doi.org/10.1038/s41477-023-01514-w

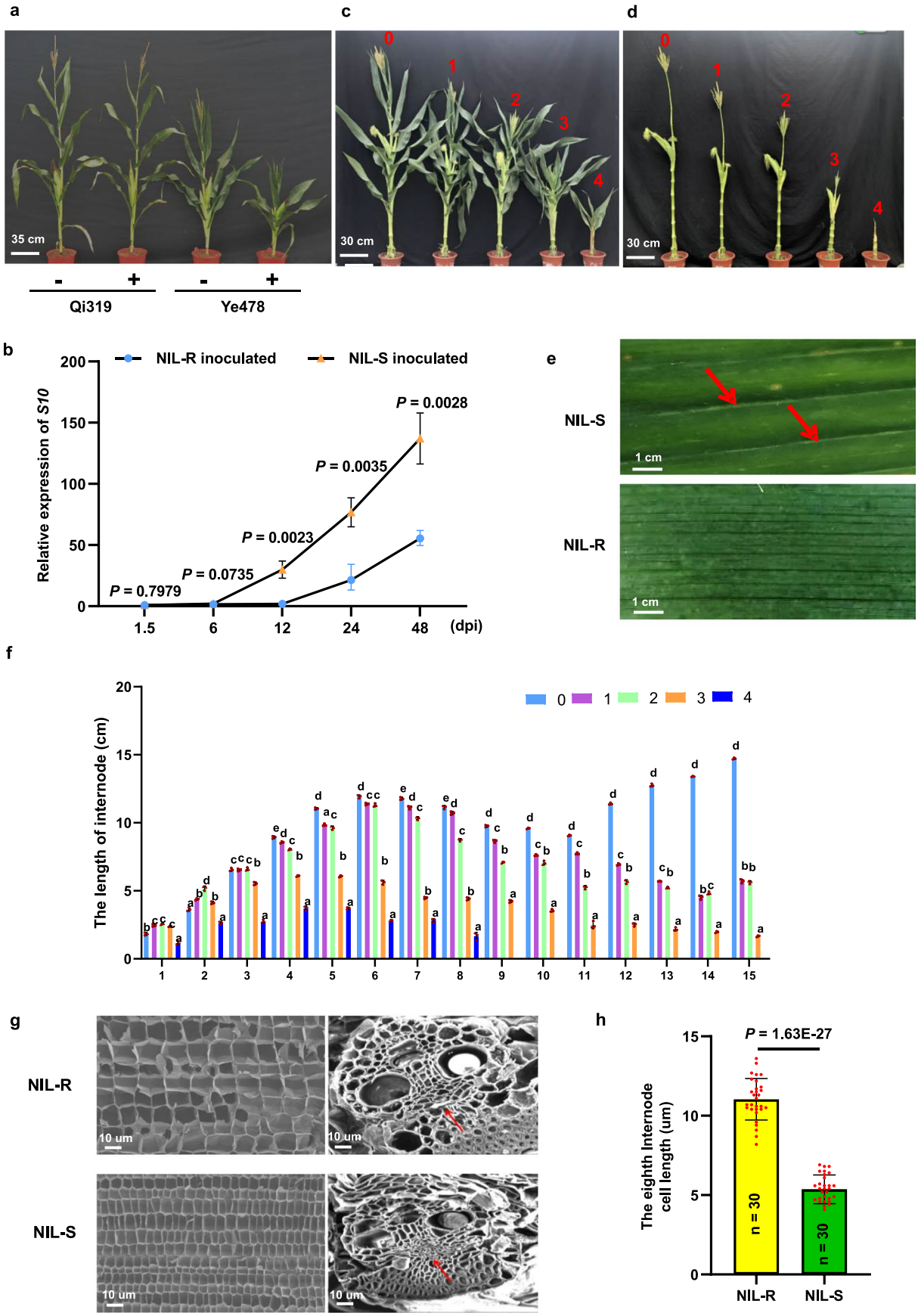

Extended Data Fig. 1 | See next page for caption.

https://doi.org/10.1038/s41477-023-01514-w

Extended Data Fig. 1 | Phenotypic and cytological characteristics of maize rough dwarf disease. a, Phenotype of Qi319 and Ye478 upon RBSDV infection. "-" represents virus-free SBPH, and "+" represents viruliferous SBPH. Scale bars, 35 cm. **b**, The relative expression of RBSDV coat protein (S10) mRNA. The values are denoted as means ± s.e.m. (n = 3 biologically independent samples). Five plants were taken as one biological replicate. **c**, **d**, The MRDD severity at the silking stage could be classified into five grades (0, 1, 2, 3, and 4) in view of the overall symptoms at the silking stage according to plant height and the characteristics of the lesions. Scale bars, 30 cm. **e**, The healthy plants (NIL-R) or severely diseased plants (NIL-S) of waxy enations on the axial surfaces of upper leaves under artificial inoculation of RBSDV. Scale bars, 1 cm. **f**, Number of internodes and length of internodes in plants with disease grades 0-4 at the silking stage. Data are means ± s.e.m. (n = 3 biologically independent samples). **g**, The left panels show the longitudinal sections of eighth internodes from the healthy NIL-R and diseased NIL-S plants. The right panels show transections of the eighth internode from the healthy NIL-R and diseased NIL-S plants. Scale bar, 10 μm. **h**, Cell length of the eighth internode between the healthy NIL-R and diseased NIL-S plants. Values are means ± SEM. (n = 30 biologically independent samples). Statistical significance was determined using two-sided Student's *t*-test. Two independent experiments were performed with similar results in g and h.

https://doi.org/10.1038/s41477-023-01514-w

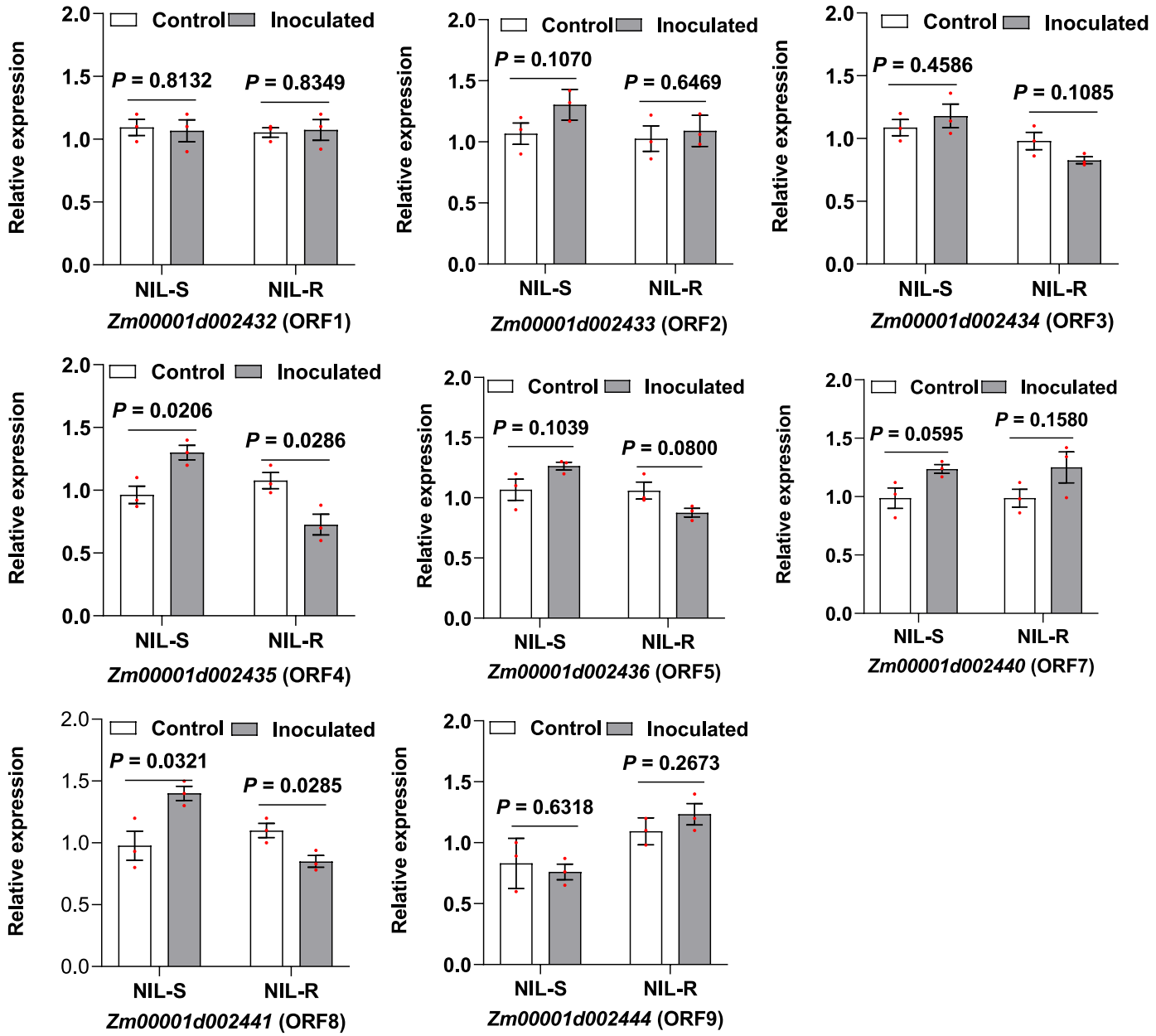

Extended Data Fig. 2 | The relative expression of candidate genes in the *qMrdd2* region. RT-qPCR assay validates the expression of candidate genes between the NIL-R and NIL-S plants under artificial inoculation of RBSDV at 12 dpi. The values are denoted as means ± s.e.m. (n = 3 independent biologically samples). Five plants were taken as one biological replicate (n = 5). Statistical significance was determined using two-sided Student's *t*-test.

https://doi.org/10.1038/s41477-023-01514-w

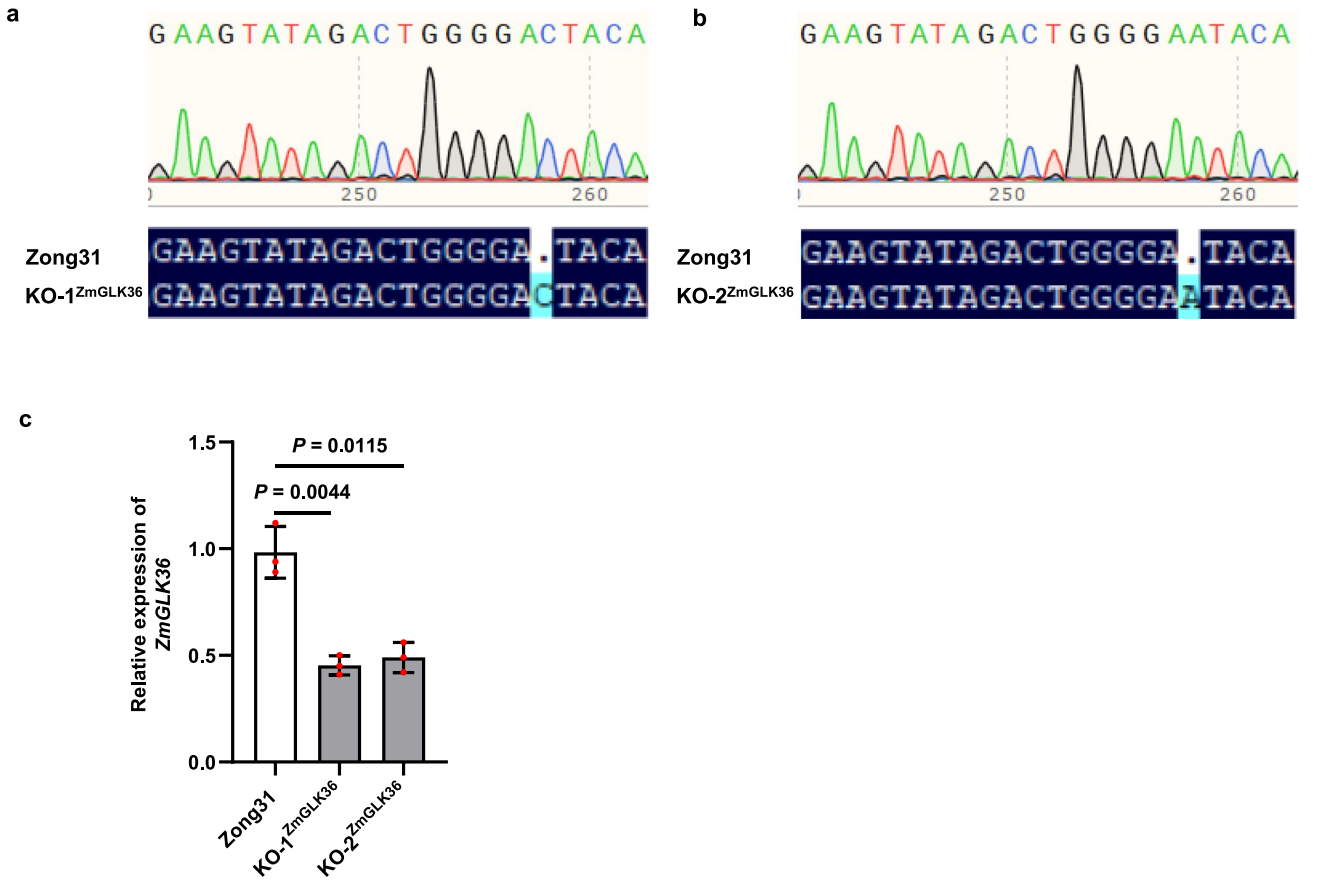

Extended Data Fig. 3 | Identification of the *ZmGLK36* knockout mutants and transgenic plants. a, b, Sequencing analysis showing mutations in the CRISPR/Cas9-generated *Zmglk36* knockout mutants. **c**, Validation of *ZmGLK36* expression in the knockout plants using RT-qPCR. The values are denoted as means ± s.e.m. (n = 3 independent biologically samples). Five plants were taken as one biological replicate (n = 5). Statistical significance was determined using two-sided Student's *t*-test.

https://doi.org/10.1038/s41477-023-01514-w

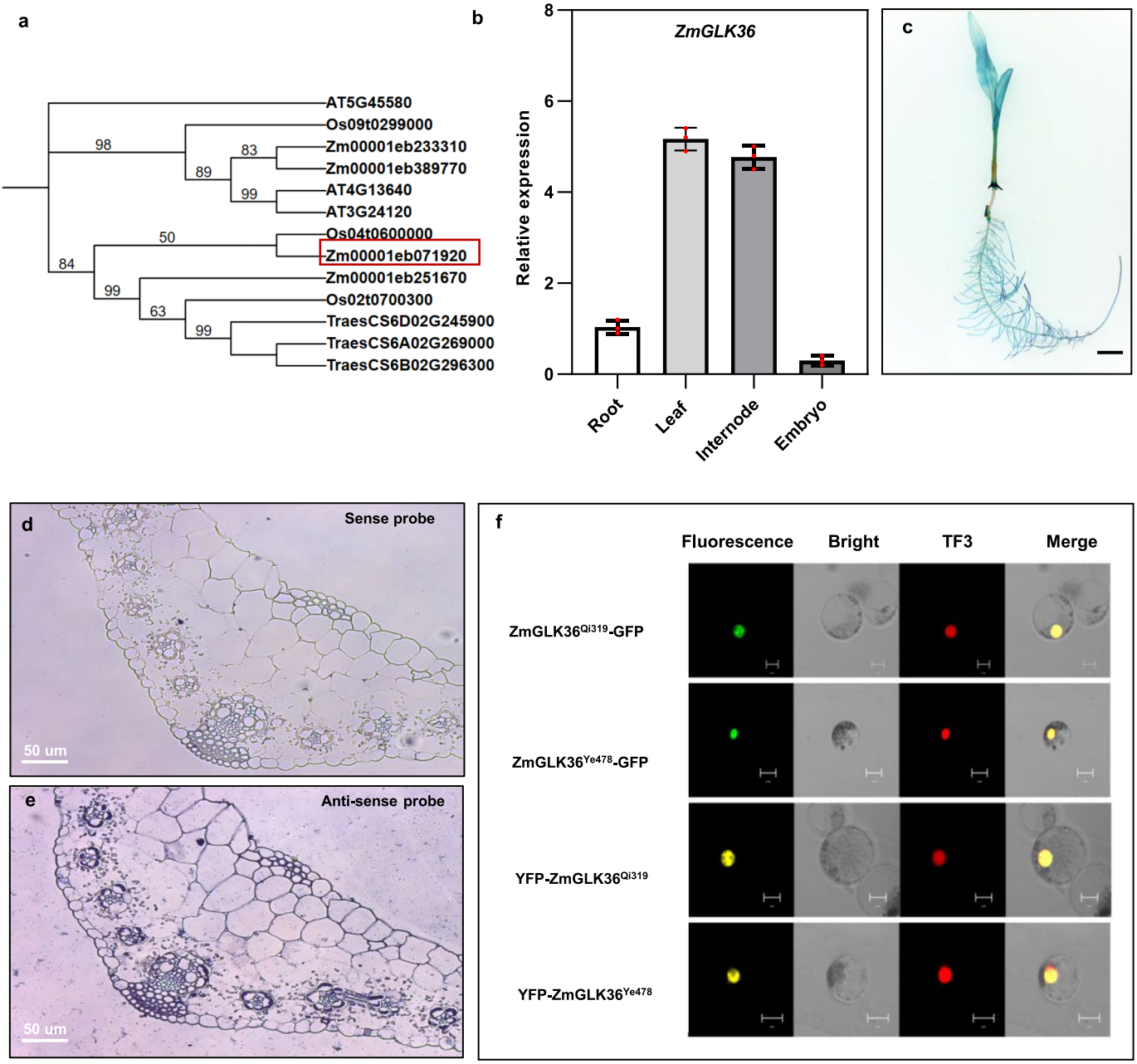

Extended Data Fig. 4 | Molecular characterization of *ZmGLK36*. **a**, Phylogenetic analysis of *ZmGLK36* and their orthologues from *Arabidopsis*, maize, rice and wheat. The phylogenetic tree was generated using the method of maximum likelihood with the MEGA7 software based on the full-length protein sequence. **b**, RT-qPCR assay showing the transcript abundance of *ZmGLK36* in various tissues. Data are means ± s.e.m. (n = 3 independent biologically samples). Five plants were taken as one biological replicate (n = 5). **c**, The expression pattern of *ZmGLK36* revealed by histochemical staining of the transgenic plants carrying a β-glucuronidase (GUS) reporter driven by the endogenous *ZmGLK36* promoter. Scale bars, 2.5 cm. **d**, **e**, RNA *in situ* hybridization analysis of *ZmGLK36* in leaf. Leaf blades of maize plants were cross-sectioned and hybridized with *ZmGLK36*-specific sense (**d**) or antisense (**e**) probes. Scale bars, 50 μm. **f**, Subcellular localization of the ZmGLK36-GFP and YFP-ZmGLK36 fusion proteins in maize protoplasts. Scale bars, 10 μm. The results are representative of three independent experiments. TF3 was used as a nuclear marker.

https://doi.org/10.1038/s41477-023-01514-w

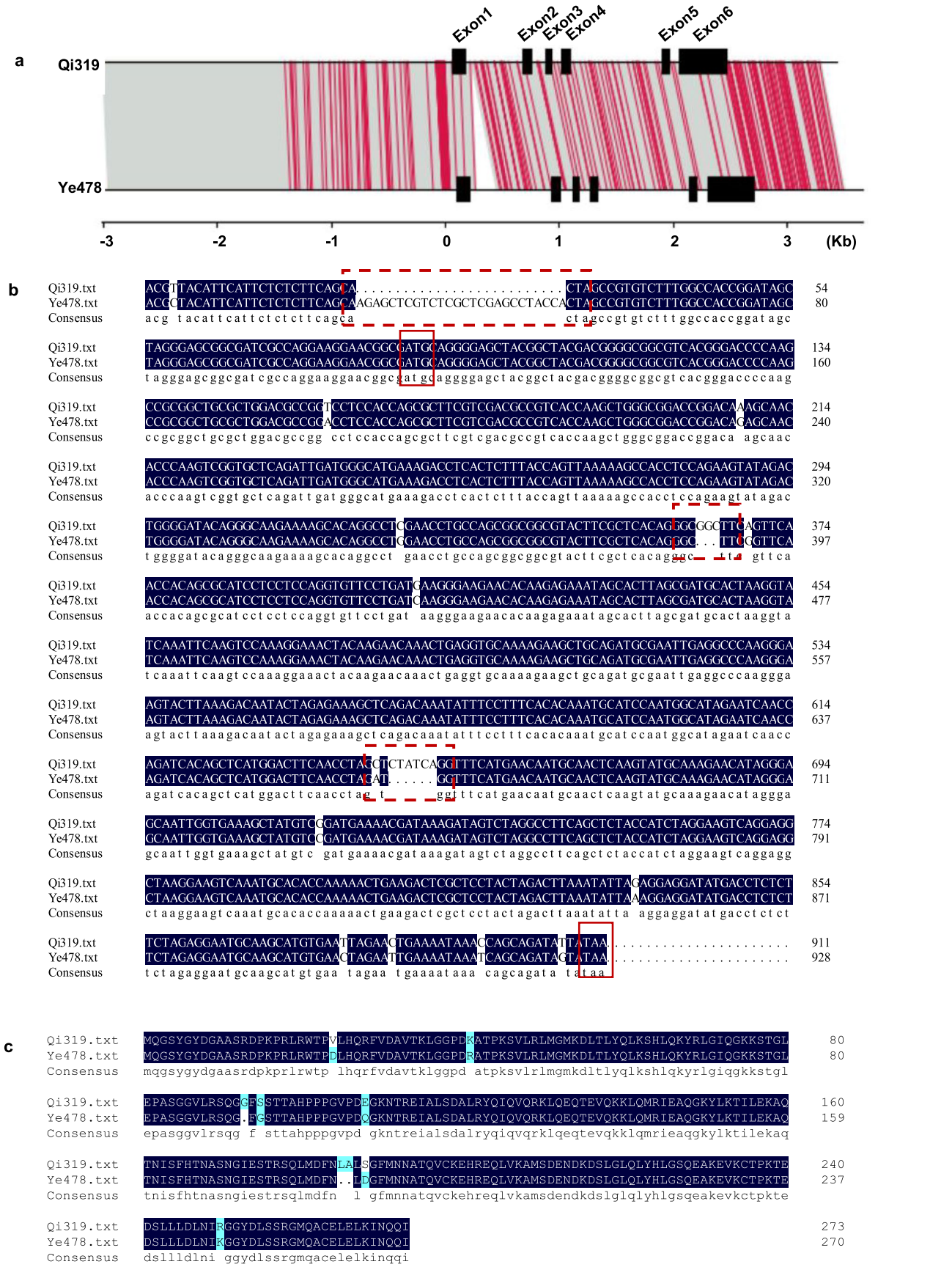

Extended Data Fig. 5 | Sequence alignment analysis of *ZmGLK36* in Qi319 and Ye478. a, Structure and sequence comparison of the *ZmGLK36* genomic region between Qi319 and Ye478. Black denotes exons. The red lines denote SNPs. **b**, Alignment of the cDNA sequences of *ZmGLK36* in Qi319 and Ye478. **c**, Amino acid sequence alignment of ZmGLK36 between Qi319 and Ye478.

https://doi.org/10.1038/s41477-023-01514-w

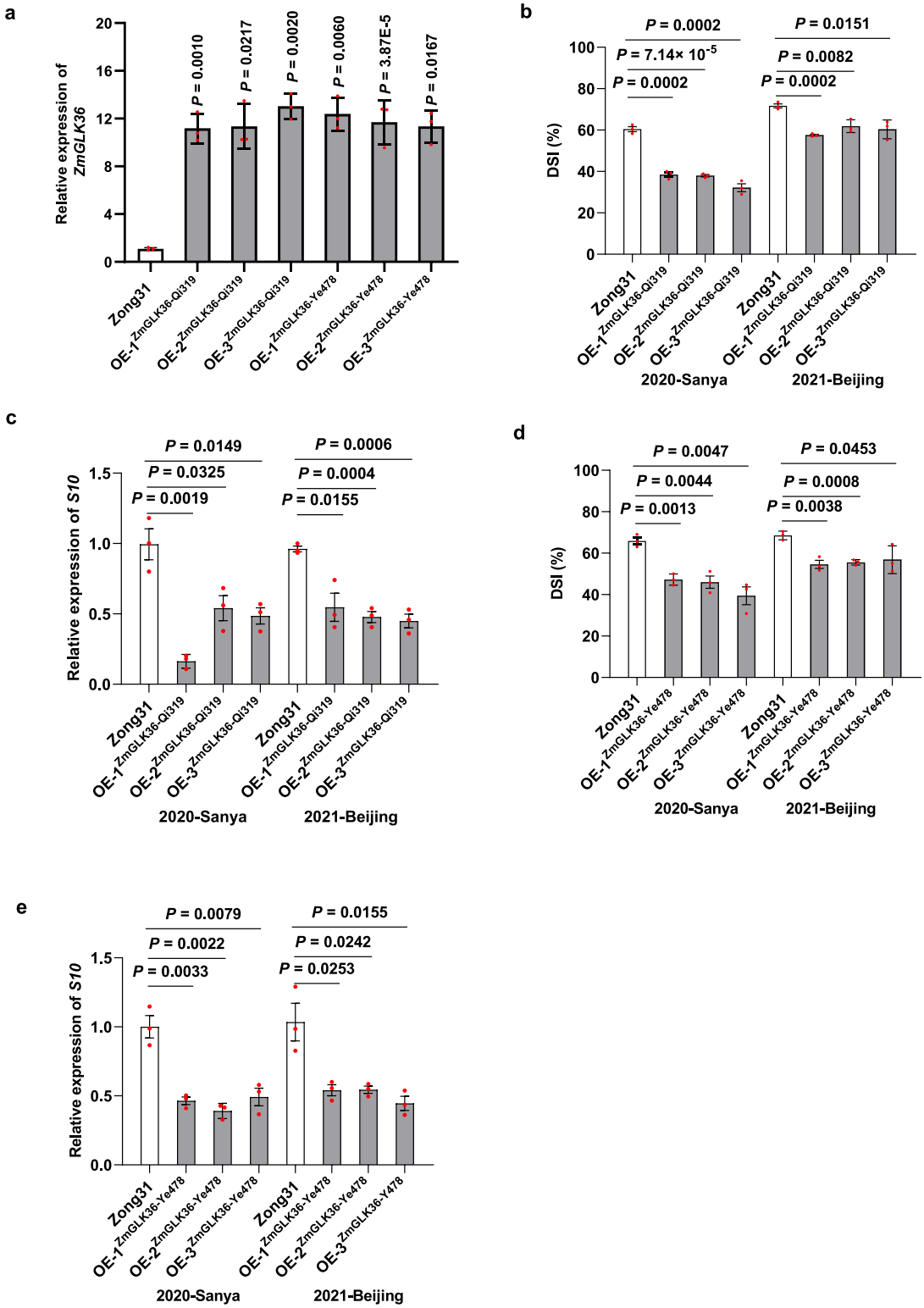

Extended Data Fig. 6 | Phenotypic examination of the *ZmGLK36* transgenic plants. a, Validation of *ZmGLK36* expression in the transgenic overexpression plants using RT-qPCR. The values are denoted as means ± s.e.m. (n = 3 independent biologically samples). **b**, **d**, The DSI values of the transgenic overexpression plants and Zong31. The plants were planted in Sanya and Beijing and used for artificial inoculation. Data are means ± s.e.m. from 3 biological replicates (n = 50 plants for each replicate). **c**, **e**, The relative expression of *RBSDV- S10* mRNA in *ZmGLK36* overexpression plants and Zong31 at anthesis. The plants were artificially inoculated at the V3 stage. The values are denoted as means ± s.e.m. from 3 biological replicates (n = 5 plants for each replicate). Statistical significance was determined using two-sided Student's *t*-test.

https://doi.org/10.1038/s41477-023-01514-w

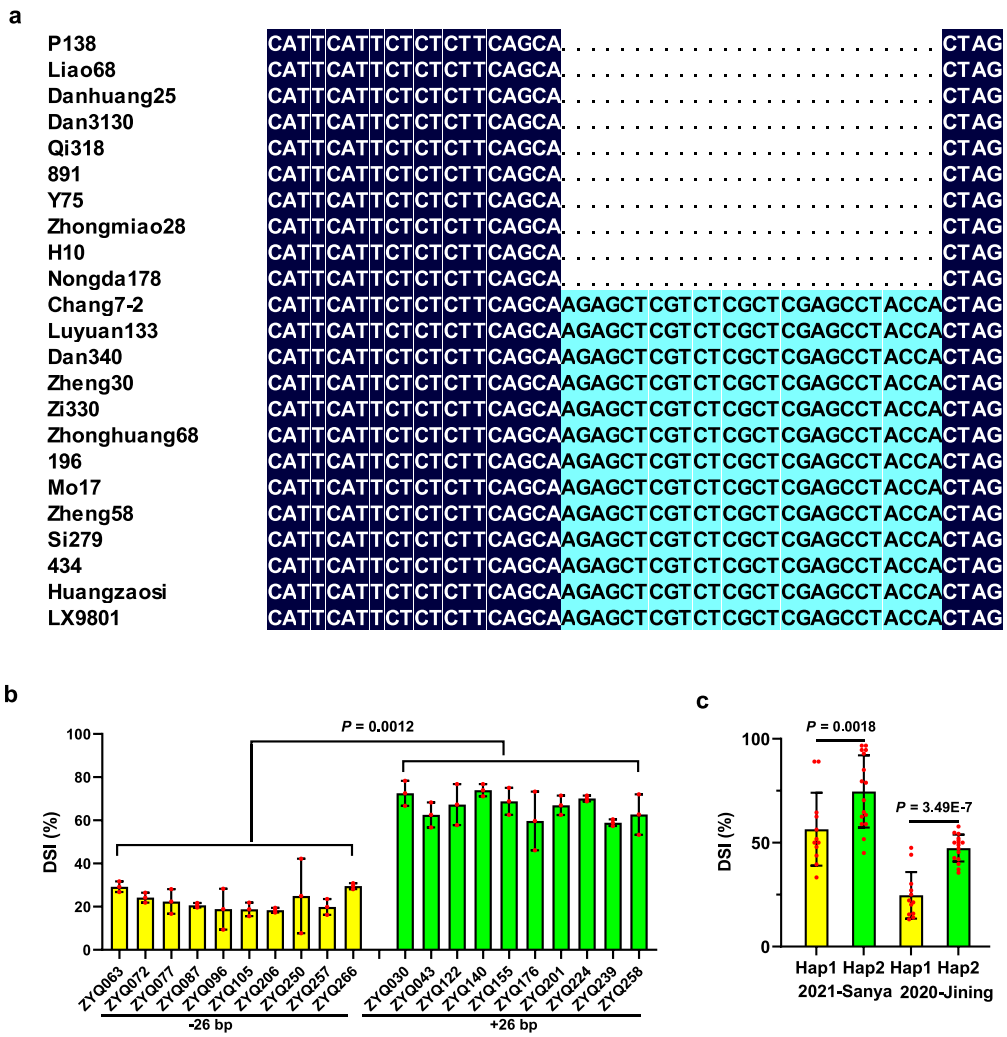

Extended Data Fig. 7 | Phenotypic analysis based on marker Indel-26. **a**, Sequence alignment analysis of 10 resistant inbred lines and 13 susceptible inbred lines from 226 temperate maize inbred lines based on the 26-bp Indel. **b**, Co-segregation analysis of the 26-bp Indel with RBSDV resistance using 20 RILs. Data are means ± s.e.m. from 3 biological replicates (n = 17 plants for each replicate). **c**, Haplotypes of *ZmGLK36* among maize germplasm from the tropical maize inbred lines based on the Indel-26. Each point represents the average DSI of two replicates from a maize inbred line. (n = 17 plants for each replicate). Statistical significance was determined using two-sided Student's t-test.

https://doi.org/10.1038/s41477-023-01514-w

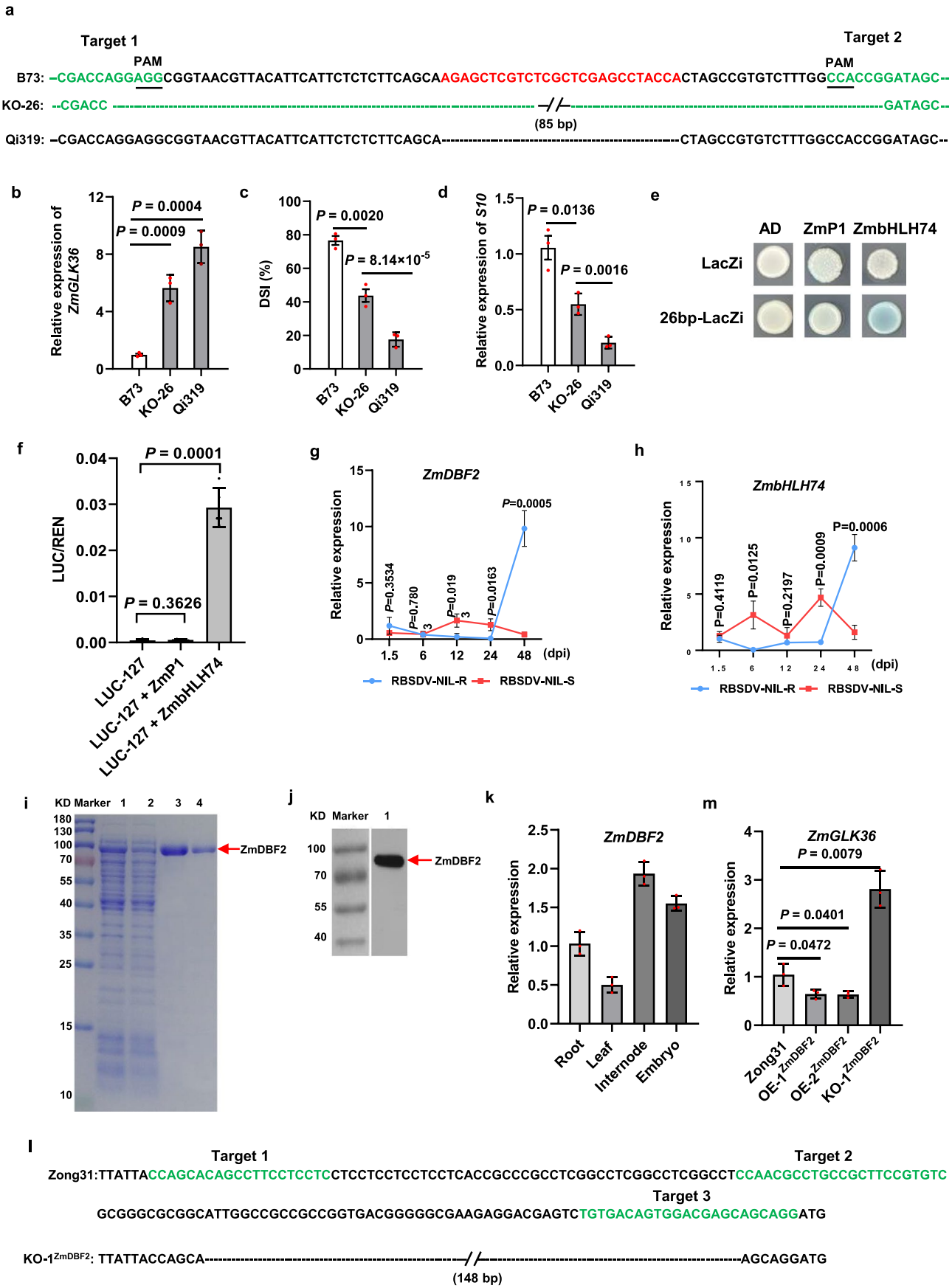

Extended Data Fig. 8 | See next page for caption.

https://doi.org/10.1038/s41477-023-01514-w

Extended Data Fig. 8 | Predicted transcription factor binding sites in the 26-bp Indel in 5'UTR of *ZmGLK36*. **a**, Diagram shows mutagenesis of the KO-26 knockout mutants. The sequence gap length is shown in parentheses. Red letters represent the 26-bp Indel. Green dashed lines indicate nucleotide deletion. **b**, Relative expression of *ZmGLK36* under RBSDV inoculation (12 dpi). The values are denoted as means ± s.e.m. (n = 3 independent biological samples). Five plants were taken as one biological replicate. Qi319 was used as the positive control. **c**, DSI values of the KO-26 plants at the silking stage. The plants were inoculated with RBSDV at the V3 stage. Data are means ± s.e.m. from 3 biological replicates (n = 34 plants for each replicate). **d**, Relative expression of RBSDV coat protein (S10) in B73, KO-26 and Qi319 plants at the silking stage. The plants were inoculated with RBSDV at the V3 stage. Data are means ± s.e.m. from 3 biological replicates (n = 5 plants for each replicate). **e**, Yeast one-hybrid (Y1H) assay shows that ZmbHLH74, but not ZmP1, binds to the 26-bp fragment. **f**, Transient transcriptional activity assay in maize protoplasts shows that ZmbHLH74, but not ZmP1, activates the LUC reporter gene expression. Values are means ± s.e.m (n = 5 repeats). **g, h**, Relative expression levels of *ZmDBF2* and *ZmbHLH74* in NIL-R and NIL-S after artificial inoculation with RBSDV. The values are denoted as means ± s.e.m. (n = 3 independent biologically samples). Each biological replicate has 5 plants. **i**, SDS–PAGE analysis of the purified MBP-ZmDBF2 recombinant protein. **j**, Western blot analysis of the purified MBP-ZmDBF2 recombinant protein by using the anti-MBP antibody. **k**, RT-qPCR assay showing the transcript abundance analysis of *ZmDBF2* in various tissues. Data are means ± s.e.m. from 3 biological replicates (n = 5 plants for each replicate). **l**, Diagram shows mutagenesis of the *ZmDBF2* knockout mutants. **m**, *ZmGLK36* transcript levels in the overexpression and KO lines of *ZmDBF2*. The values are denoted as means ± s.e.m. from 3 biological replicates (n = 5 plants for each replicate). Statistical significance was determined using a two-sided *t*-test. The experiments in i, and j were independently performed two times with similar results.

https://doi.org/10.1038/s41477-023-01514-w

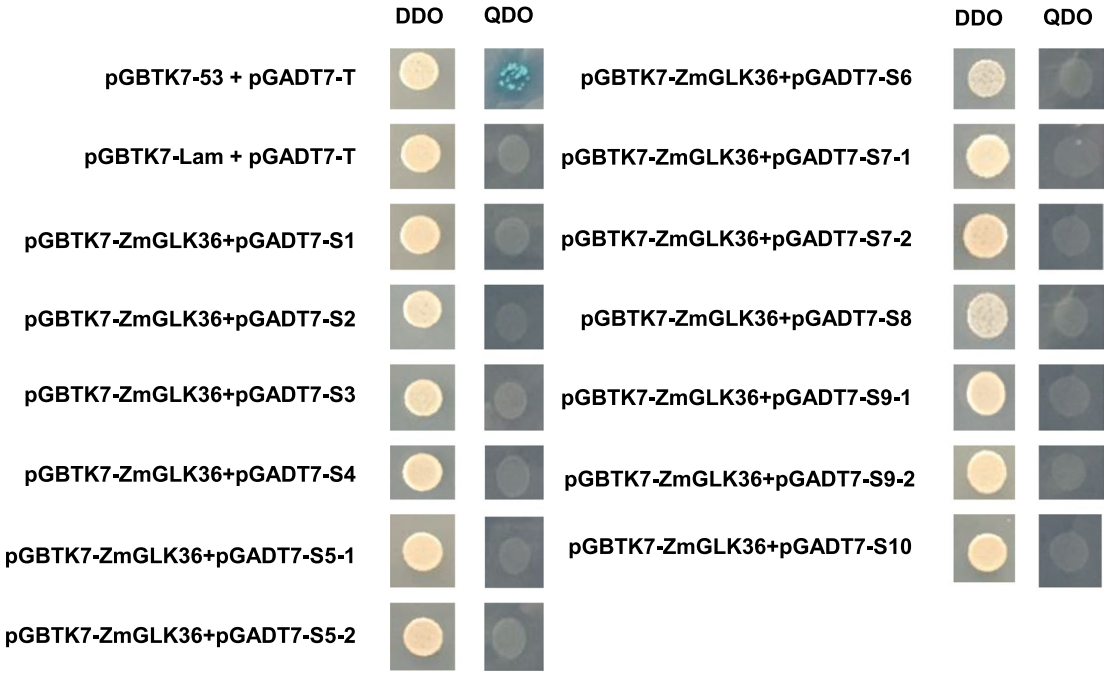

Extended Data Fig. 9 | Yeast two-hybrid assay of the interaction between ZmGLK36 and RBSDV proteins. Yeast two-hybrid (Y2H) assay shows that there is no direct interaction between ZmGLK36 and RBSDV proteins (S1, S2, S3, S4, S5-1, S5-2, S6, S7-1, S7-2, S8, S9-1, S9-2 and S10).

https://doi.org/10.1038/s41477-023-01514-w

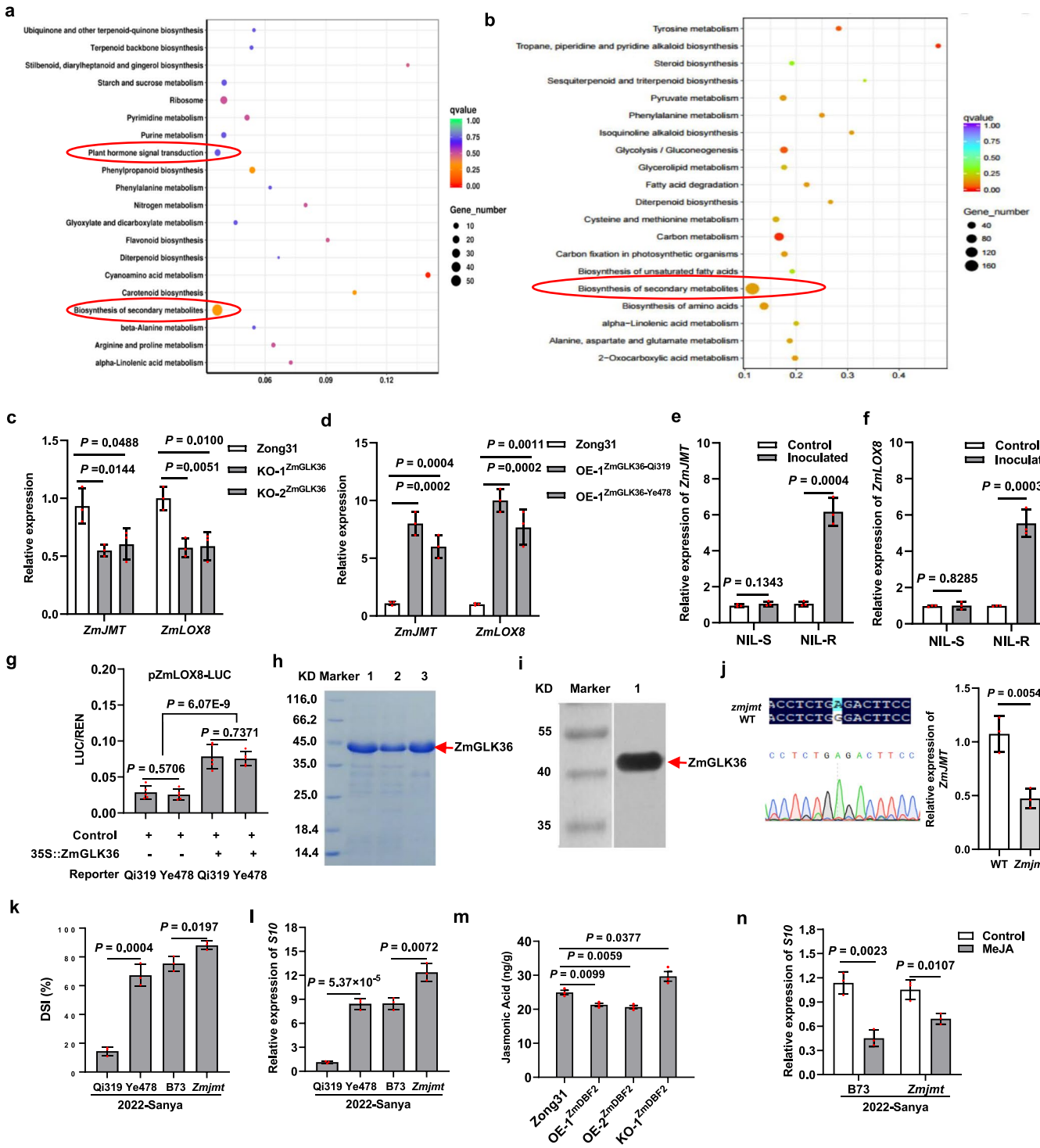

Extended Data Fig. 10 | See next page for caption.

https://doi.org/10.1038/s41477-023-01514-w

Extended Data Fig. 10 | ZmGLK36 entails the JA signaling pathway for resistance to RBSDV. a, KEGG estimation of the RNA_seq data based on Zong31 and *ZmGLK36* overexpressing plants under nonpathogenic stress conditions. **b**, KEGG estimation of the RNA_seq data based on NIL-R (inoculation of non-toxic SBPH) and NIL-R (inoculation of poisonous SBPH). **c**, **d**, RT-qPCR assay showing the transcript abundance analysis of *ZmJMT* and *ZmLOX8* in Zong31, KO-1^{ZmGLK36}, KO-2^{ZmGLK36}, OE-1$^{ZmGLK36\text{-}Qi319}$ and OE-1$^{ZmGLK36\text{-}Ye478}$. Data are means ± s.e.m. from 3 biological replicates (n = 5 plants for each replicate). **e**, **f**, Relative expression of *ZmJMT* and *ZmLOX8* in NIL-S and NIL-R under artificial inoculation with RBSDV. Data are means ± s.e.m. from 3 biological replicates (n = 5 plants for each replicate). **g**, Transient transcriptional activity assay in maize protoplasts shows that ZmGLK36 activates *ZmLOX8* expression. Values are means ± s.e.m (n = 5 repeats). **h**, SDS–PAGE analysis of the purified His-ZmGLK36 recombinant protein. **i**, Western blot analysis of the purified His-ZmGLK36 recombinant protein by using the anti-His antibody. **j**, The left is sequencing peak diagram of premature termination of mutants. The right is relative expression of *ZmJMT* in wild type (B73) and *Zmjmt* mutants. Data are means ± s.e.m. from 3 biological replicates (n = 5 plants for each replicate). **k**, DSI values of Qi319, Ye478, B73 and *Zmjmt* mutant plants at the salking stage. Data are means ± s.e.m. from 3 biological replicates (n = 34 plants for each replicate). **l**, Relative expression of RBSDV-S10 mRNA in B73 and *Zmjmt* mutant plants at the at the silking stage. The values are denoted as means ± s.e.m. from 3 biological replicates (n = 5 plants for each replicate). **m**, Determination of JA content in Zong31, transgenic overexpression and knockout plants of *ZmDBF2*. Data are means ± s.e.m. from 3 biological replicates (n = 5 plants for each replicate). **n**, RT-qPCR analysis of RBSDV-S10 mRNA accumulation in RBSDV-infected maize leaves pretreated with MeJA. Data are means ± s.e.m. from 3 biological replicates (n = 5 plants for each replicate). Statistical significance was determined using two-sided Student's *t*-test. The experiments in h, and i were independently performed two times with similar results.

nature portfolio

Corresponding author(s): XinhaiLi

Last updated by author(s): Aug 1, 2023

Reporting Summary

Nature Portfolio wishes to improve the reproducibility of the work that we publish. This form provides structure for consistency and transparency in reporting. For further information on Nature Portfolio policies, see our Editorial Policies and the Editorial Policy Checklist.

Statistics

For all statistical analyses, confirm that the following items are present in the figure legend, table legend, main text, or Methods section.

n/a	Confirmed
☐	☒ The exact sample size (*n*) for each experimental group/condition, given as a discrete number and unit of measurement
☐	☒ A statement on whether measurements were taken from distinct samples or whether the same sample was measured repeatedly
☐	☒ The statistical test(s) used AND whether they are one- or two-sided *Only common tests should be described solely by name; describe more complex techniques in the Methods section.*
☒	☐ A description of all covariates tested
☒	☐ A description of any assumptions or corrections, such as tests of normality and adjustment for multiple comparisons
☐	☒ A full description of the statistical parameters including central tendency (e.g. means) or other basic estimates (e.g. regression coefficient) AND variation (e.g. standard deviation) or associated estimates of uncertainty (e.g. confidence intervals)
☐	☒ For null hypothesis testing, the test statistic (e.g. *F*, *t*, *r*) with confidence intervals, effect sizes, degrees of freedom and *P* value noted *Give P values as exact values whenever suitable.*
☒	☐ For Bayesian analysis, information on the choice of priors and Markov chain Monte Carlo settings
☐	☒ For hierarchical and complex designs, identification of the appropriate level for tests and full reporting of outcomes
☒	☐ Estimates of effect sizes (e.g. Cohen's *d*, Pearson's *r*), indicating how they were calculated

Our web collection on statistics for biologists contains articles on many of the points above.

Software and code

Policy information about availability of computer code

Data collection	ABI 7500 real-time detection system (Applied Biosystems) was used to collect RT-qPCR raw data. Confocal laser-scanning microscope (TCS SP5; Leica), S-3400N Hitachi scanning electron microscope for photographing (Hitachi High Technologies, Tokyo, Japan) and Leica DMR microscope (Leica DM5000B and a camera fitted with a Micro Color CCD (Apogee Instruments) were used to image capture and display. The Qi319 library was constructed and sequenced using the Pacific Bioscience Sequel II platform (Annoroad Gene Technology). Promega GloMaxTM96 Instrument (Promega) was used for relative fluorescence activity. LC-MS/MS (QTRAP 6500+,SCIEX) was used to determine JA content. The Ultra Performance Liquid Chromatography (UPLC, SHIMADZU Nexera X2) and Tandem mass spectrometry (Applied Biosystems 4500 QTRAP) was used to data acquisition of metabolites.
Data analysis	TASSEL V5.0 was used to analyze the association between these variations and resistance to RBSDV. MEGA V5.0 and DNAMAN (version 5.2.2) were used to align DNA sequence. Excel 2016 (Microsoft) and GraphPad Prism (version 8.0.1) was used to perform gene expression analysis and statistical analysis. The code reference for transcriptome data analysis is as follows:https://github.com/wangtao-go/fpkm/blob/main/calRPKM.pl. The annotation pipeline for prediction of repeat elements includes de novo and homology-based approaches. For homolog evidence, alignment searches were undertaken against the RepBase database (http://www.girinst.org/repbase), and then were predicted by Repeat Protein Mask (http://www.repeatmasker.org/). For de novo annotation, LTR_FINDER, PILER, RepeatScout (http://www.repeatmasker.org/), and Repeat-Modeler (v2.0.3) (http://www.repeatmasker.org/RepeatModeler.html) were used to construct a de novo library, then annotation was carried out with Repeat masker (v4.1.2) (http://repeatmasker.org/). Sequence analysis via PlantPAN 3.0 TF URL (http://plantpan.itps.ncku.edu.tw/).

For manuscripts utilizing custom algorithms or software that are central to the research but not yet described in published literature, software must be made available to editors and reviewers. We strongly encourage code deposition in a community repository (e.g. GitHub). See the Nature Portfolio guidelines for submitting code & software for further information.

Data

Policy information about availability of data

All manuscripts must include a data availability statement. This statement should provide the following information, where applicable:

- Accession codes, unique identifiers, or web links for publicly available datasets
- A description of any restrictions on data availability
- For clinical datasets or third party data, please ensure that the statement adheres to our policy

The datasets generated and/or analyzed during the current study are attached. Any additional data are available from the corresponding author. No participant identifiable information will be disclosed.

Research involving human participants, their data, or biological material

Policy information about studies with human participants or human data. See also policy information about sex, gender (identity/presentation), and sexual orientation and race, ethnicity and racism.

Reporting on sex and gender	N/A
Reporting on race, ethnicity, or other socially relevant groupings	N/A
Population characteristics	N/A
Recruitment	N/A
Ethics oversight	N/A

Note that full information on the approval of the study protocol must also be provided in the manuscript.

Field-specific reporting

Please select the one below that is the best fit for your research. If you are not sure, read the appropriate sections before making your selection.

☒ Life sciences ☐ Behavioural & social sciences ☐ Ecological, evolutionary & environmental sciences

For a reference copy of the document with all sections, see nature.com/documents/nr-reporting-summary-flat.pdf

Life sciences study design

All studies must disclose on these points even when the disclosure is negative.

Sample size	Three biological replicates for Metabolomics and RNA-seq analyses, following the common practice in the field. RT-qPCR, each experiment was analyzed at least with three biological replicates. Each biological replicate at least has 5 plants. For the statistics of JA content, we performed at least three independent biological replicates. DSI data of transgenic plant were performed at least three independent biological replicates and collected from at least 34 plants/genotype as one biological replicate. DSI data of maize inbred lines and hybrids collected from at least 17 plants/genotype as one biological replicate. Sample sizes are indicated in the main text, figures and legends. We confirmed that the sample sizes that we used in this study were adequate by performing biological replicates and obtaining similar results. Sample sizes for validations are listed in the figures and based on previous studies (Liu, et al., 2020. A helitron-induced RabGDIα variant causes quantitative recessive resistance to maize rough dwarf disease. Nat Commun. 11(1):495. doi: 10.1038/s41467-020-14372-3; Jiang, et al., 2022. Natural polymorphism of ZmICE1 contributes to amino acid metabolism that impacts cold tolerance in maize. Nat Plants. 28(10):1176-1190. doi: 10.1038/s41477-022-01254-3.).
Data exclusions	No data were excluded from our analyses.
Replication	All experiments were replicated independently and performed at least two with similar results. Number of repeats is provided in the figure legends where appreciate.
Randomization	A randomized complete block design was used in all trials for phenotype collection.
Blinding	The investigators were blinded to group allocation during data analysis.

Reporting for specific materials, systems and methods

We require information from authors about some types of materials, experimental systems and methods used in many studies. Here, indicate whether each material, system or method listed is relevant to your study. If you are not sure if a list item applies to your research, read the appropriate section before selecting a response.

Materials & experimental systems

n/a	Involved in the study
☐	☒ Antibodies
☒	☐ Eukaryotic cell lines
☒	☐ Palaeontology and archaeology
☒	☐ Animals and other organisms
☒	☐ Clinical data
☒	☐ Dual use research of concern
☒	☐ Plants

Methods

n/a	Involved in the study
☒	☐ ChIP-seq
☒	☐ Flow cytometry
☒	☐ MRI-based neuroimaging

Antibodies

Antibodies used

The information of the antibodies used in this study was shown below:
Mouse monoclonal anti His (named:Anti His mAb) (Zoonbio Biotechnology Co.,Ltd, Nanjing, China; Cat#ABM-0008; 1:1000);
Mouse monoclonal anti MBP (named:MBP-Tag(4M14) Mouse mAb) (Abmart, Beijing, China; Cat#M20051H; 1:2000);

Validation

http://www.zoonbio.com/pruduct/his-antibody-0008.html
http://www.ab-mart.com.cn/product.aspx